



Title	Phase-Separation Induced Circular Dichroism of Optically Active Polyfluorene Derivatives
Author(s)	Sanada, Yusuke
Citation	大阪大学, 2011, 博士論文
Version Type	VoR
URL	https://hdl.handle.net/11094/26856
rights	
Note	

The University of Osaka Institutional Knowledge Archive : OUKA

<https://ir.library.osaka-u.ac.jp/>

The University of Osaka

現中 1518.8

Phase-Separation Induced Circular Dichroism
of Optically Active Polyfluorene Derivatives

A Doctoral Thesis

By

Yusuke Sanada

Submitted to the Graduate School
of Science, Osaka University

August, 2011

Phase-Separation Induced Circular Dichroism
of Optically Active Polyfluorene Derivatives

(光学活性ポリフルオレン誘導体の
相分離誘起円二色性)
A Doctoral Thesis

By

Yusuke Sanada

Submitted to the Graduate School
of Science, Osaka University

August, 2011

Acknowledgements

All works of this thesis was carried out from 2008 to 2011 under the direction of Professor Takahiro Sato at Department of Macromolecular Science, Graduate School of Science, Osaka University. I thank Professor Takahiro Sato for his guidance, advice, and encouragement throughout the course of this work.

My sincere appreciation is extended to Dr. Akihito Hashidzume and Dr. Ken Terao of the Osaka University for their helpful advice and valuable discussion.

I am very grateful to Professor Kazuo Sakurai and Dr. Isamu Akiba of the University of Kitakyushu for their helpful advice and supports for X-ray scattering measurements.

The synchrotron radiation experiments were performed at the BL40B2 of SPring-8 with the approval of the Japan Synchrotron Radiation Research Institute (JASRI) (Proposal No. 2010A1432).

This work was partly supported by a Grant-in-Aid for Scientific Research on Priority Area “Soft Matter Physics”. I also acknowledge the financial support (2008-2010) from the global center of excellence program, “Global Education and Research Center for Bio-Environmental Chemistry” of Osaka University.

I thank all the members of Sato’s and Norisuye’s laboratories for their friendships.

Finally I would like to thank my parents Yoshiaki and Chiharu Sanada for their constant encouragement.

Kitakyushu, Fukuoka

August, 2011

真田 雄介

Yusuke Sanada

Contents

Chapter 1

General Introduction

1.1 Research History of Conjugated Polymer Syntheses	1
1.2 Electrical and Optical Properties of Organic Semiconductors	2
1.3 Helicity of Conjugated Polymers	5
1.4 Study of Polyfluorenes	11
1.5 Purpose of This Study	14
1.6 References	16

Chapter 2

Phase-Separation Induced Circular Dichroism in Dilute Solutions of an Optically Active Polyfluorene Homopolymer

2.1 Introduction	22
2.2 Experimental Section	
2.2.1 Polymer Samples	24
2.2.2 Turbidity	25
2.2.3 Circular Dichroism and UV-VIS Absorption	25
2.2.4 Light Scattering	26
2.3 Results and Discussion	
2.3.1 Phase Diagram	29

2.3.2 Circular Dichroism and UV-VIS Absorption	30
2.3.3 Light Scattering	35
2.3.4 Intermolecular Chiral Interaction and CD Induction	41
2.4 Conclusions	46
2.5 References	47

Chapter 3.

Double Screw-Sense Inversions of Helical Chiral-Achiral Random Copolymers of Fluorene Derivatives in Phase Separating Solutions

3.1 Introduction	52
3.2 Experimental Section	
3.2.1 Samples	54
3.2.2 Measurements	56
3.3 Results	
3.3.1 Static Light Scattering	56
3.3.2 Circular Dichroism Induction	58
3.4 Discussion	62
3.5 Conclusions	68
3.6 References	69

Chapter 4.

X-Ray Scattering Study on Concentrated Solutions of Polyfluorene

Derivatives

4.1 Introduction	75
4.2 Experimental Section	
4.2.1 Polymer Samples	76
4.2.2 Preparation of Dilute THF Solutions	76
4.2.3 Preparation of a Precipitate from a Methanol-Added THF Solution	76
4.2.4 Preparation of Concentrated Mesitylene Solutions	77
4.2.5 X-ray Scattering	77
4.2.6 CD and UV-VIS Measurements	78
4.3 Results and Discussion	
4.3.1 CD and UV-VIS Spectra of the Concentrated Solution	78
4.3.2 X-ray Scattering Profiles	79
4.4 Conclusion	86
4.5 References	87

Chapter 5.

Summary and Conclusions	89
-------------------------	----

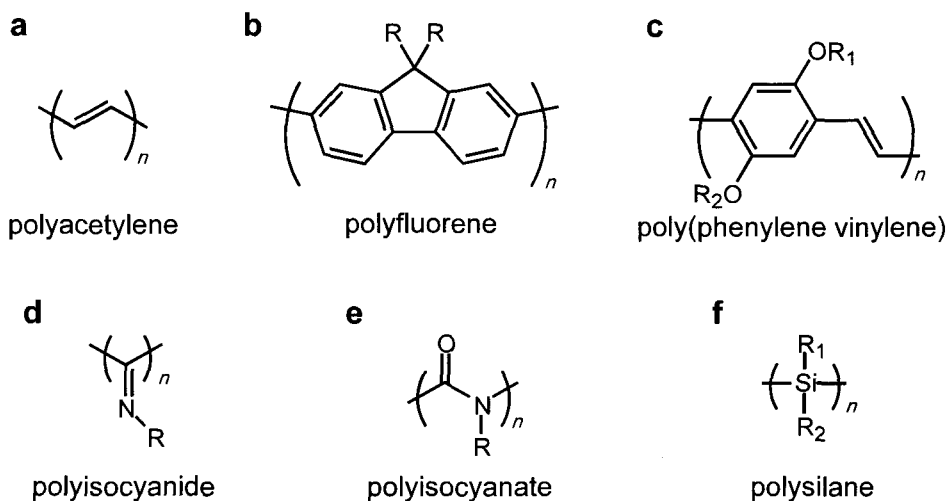
Chapter 1.

General Introduction

1.1 Research History of Conjugated Polymer Syntheses

In 1950's, Ziegler and Natta found a new polymerization catalyst based on titanium compounds combined with organoaluminum compounds.^{1,2} This noble catalyst enables us to polymerize acetylene, triggering the study for conjugated polymers. Polyacetylene (cf. Scheme 1-1a) attracted a great deal of attention as a candidate of electrically conductive materials, but the Ziegler-Natta catalyst produced only insoluble and infusible powder samples, which is hard to use as electrical materials. In 1960's, Shirakawa et al. succeeded to make film samples of polyacetylene using an excess amount of Ziegler-Natta catalyst.^{3,4} The polyacetylene film showed high conductivity after doping with iodine vapor,⁵ and is known as the first example of π -conjugated conductive polymers. For this achievement, Shirakawa won the Nobel Prize in Chemistry together with Alan U. Heeger and Alan G. MacDiarmid.

In 1979, Suzuki et al. developed cross coupling reactions which can easily make carbon-carbon covalent bonding in organic reactions.⁶ It is still fresh in our memory that Suzuki et al. won the Nobel Prize in Chemistry for this achievement. In polymer chemistry this technique allows us to make bonding between two aromatic rings, and various π -conjugated



Scheme 1-1. Chemical structures of polymers appearing in this Chapter.

polymers, such as polyfluorenes⁷ and poly(phenylene vinylene)s (cf. Scheme 1-1b and c), were synthesized using this reaction technique. A lot of studies were carried out not only for cross coupling but also homo coupling with various metal catalysts or reagents (palladium complexes⁸ or nickel reagents^{9,10}), and various kinds of monomers were combined to synthesize new π -conjugated polymers.

1.2 Electrical and Optical Properties of Organic Semiconductors

Since 1960's, not only polymeric organic semiconductors but also semiconducting small molecules have been developed extensively.¹¹ Semiconductivity of these organic materials mainly arises from hole and electron conduction layers separated by a band gap, being similar to that for inorganic semiconductors. Characteristic features of the organic

semiconductors are their processability, mechanical flexibility, and low cost. These materials are expected to use as light-emitting diodes, solar cells, field-effect transistors, and also chemical and bio-sensors. Among them, π -conjugated polymers have potential applications to printing electric circuits, flexible transparent displays or conductors, and actuators. The conjugated polymers themselves have low electric conductivity, but oxidative doping with e.g., halogens increases the conductivity enormously. In 1970's, the addition of a various kind of dopants improved electronic conductivity of π -conjugated materials. Techniques of the purification and doping are important in the application to electronic materials.¹²

π -Conjugated polymers have alternating single and double bonds in main chain. All carbon atoms of main chains has π -electron, and if bonds of a main chain take planer structure, adjacent π -orbital overlaps each other and π -electron may move along the main chain freely. Furthermore, delocalization reduces the excitation energy level, and π -electron can be excited by absorption of light with long wavelengths. Due to this low-energy excitation, conjugated polymers can be used as photo cells¹³ and light-emitting diodes,¹⁴ like inorganic semiconductor. The behavior of the π -electron described above results in the characteristic electrical and optical properties.

Processability and flexibility are characteristic features of conductive polymers distinguished from inorganic metals or semiconductors.^{15,16}

However, the processability and flexibility often need introduction of proper side chains to π -conjugated polymers.¹⁷ On the other hand, the introduction of the side chain may disturb the planarity or conjugation of the main chain. Therefore, suitable molecular designs are necessary to obtain high performance conductive polymers. The selection of the side chain is also important to tune, the wavelength of absorbed and emitted light.

Optical properties of polyisocyanides and polyisocyanates (cf. Scheme 1-1d and e) resemble those of the π -conjugated hydrocarbon polymers. Main chains of polyisocyanates¹⁸ and polyisocyanides¹⁹ consist of alternating carbonyl carbon atoms and nitrogen atoms and of carbon atoms double bonded with nitrogen atoms, respectively, and π -electrons on the main chains play an essential role in their optical properties.

We can add polysilane and its derivatives (cf. Scheme 1-1f) to conjugated polymers. Although the main chain of polysilanes consist of singly bonded silicon atoms, σ -bond electrons of silicon atoms can delocalize to reduce the excitation energy level. For this reason, polysilanes are referred to as σ -conjugated polymers. The main chain of polysilane has a narrow UV absorption band near 300 nm and is called the one-dimensional semiconductor on the analogy of three-dimensional silicon crystals used as semiconductors.²⁰ However, polysilanes decompose easily by light irradiation, which is the disadvantage in the use as

conducting and semiconducting materials.

1.3 Helicity of Conjugated Polymers

As mentioned above, the main chain of π -conjugated polymers tends to take the planer conformation since the overlapping of π -orbitals of neighboring carbon atoms stabilizes the bonding energy. However, as shown in Figure 1-1, the planer conformation often brings about steric repulsion between adjacent side chains. To escape the steric repulsion, the internal rotation of the main chain must slightly deviate from the planer conformation, but the deviation should be minimized to keep the π -orbital overlapping. As the result, each main chain bond takes a fixed tilted rotational angle, and π -conjugated polymers take a certain helical conformation. Stable helical conformations of polyacetylene, as well as of polyisocyanate and polyisocyanide, arise from this mechanism.

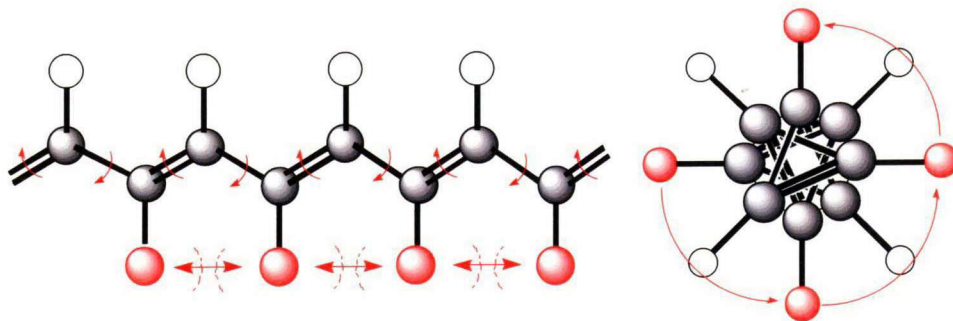


Figure 1-1. Schematic illustrations of a π -conjugated polymer and of the helical conformation formed by escaping the steric repulsion between side chains.

Such a π -conjugated polymers takes two kinds of helical states, i.e., the right- and left-handed states, which have the opposite sign but the same magnitude of the internal rotation angle of main chain. If the side chain or chain end(s) of the π -conjugated polymer has no chirality, the right- and left-handed helical states should appear with equal probability so that the helical π -conjugated polymer must be racemic. On the other hand, if the π -conjugated polymer has optically active side chains (or chain ends) or is dissolved in a chiral solvent, the right- and left-handed helical states may be distinguished each other and the polymer exhibits strong circular dichroism (CD) in the wavelength region of UV-visible absorption of its main chain.

If the helix sense is often inverted along the main chain, the polymer should not be regarded as a helical polymer. In fact, most of helical polymers have long sequences of one sense helical state and the helix reversal seldom occurs in their main chain. As explained below, the difficulty in the helix reversal amplifies the discrimination of right- and left-handed helical states in the whole polymer chain, and brings about cooperativity in the helical conformation which is reflected on interesting CD or optical rotation behavior (see below) and nonlinear responses to chiral external stimuli.

Let consider a helical polymer chain of which monomer unit can take only the right- and left-handed helical states (the P and M states,

respectively). Energies of the P and M states per monomer unit are denoted as E_P and E_M , respectively, and the latter is selected as the reference energy, setting $E_M = 0$. As shown in Figure 1-2, it is assumed that E_P is much lower than the thermal energy, represented by the product of the Boltzmann constant k_B and the absolute temperature T , and furthermore that the helix reversal requires additional energy E_r being much higher than the thermal energy; i.e., $E_P \ll k_B T$ and $E_r \gg k_B T$. On these assumptions, the dimer takes the P and M states with almost the even probability due to the thermal agitation, but the helix reversal hardly occurs.

Under these conditions, if the degree of polymerization N increases,

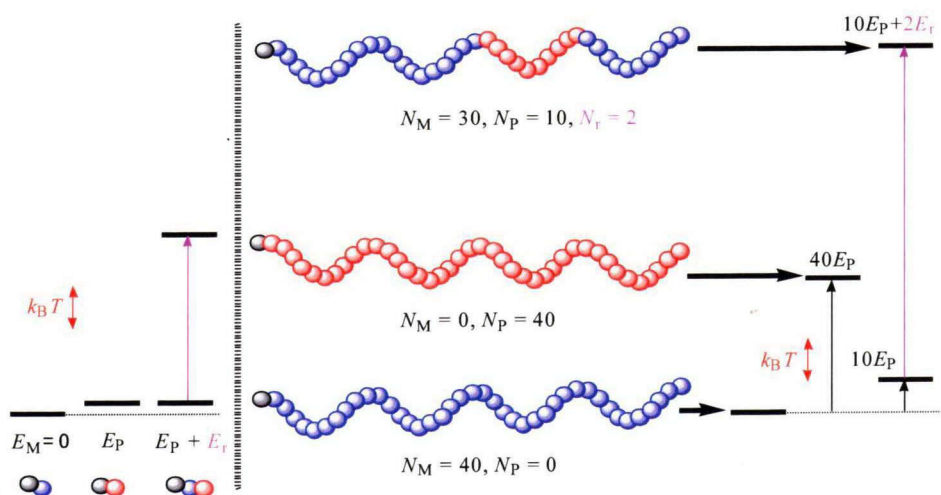


Figure 1-2. Energy levels of the perfect M and P helices and of an imperfect helical state containing a helix reversal. Red and blue circles indicate monomers taking the P and M states, respectively.

the energy difference between the perfect P and M helices increases proportionally with N , as illustrated in Figure 1-2. When NE_p becomes much higher than $k_B T$, the perfect P helix seldom appears in comparison with the perfect M helix. On the other hand, imperfect helical states containing helix reversals also seldom appear because of high E_r . Therefore, only the perfect M helix is the stable conformation in the polymer chain. We can say that monomer units with the small energy difference E_p cooperate in the polymer chain to discriminate the right- and left-handed helical states. This is the origin of cooperativity of the helical polymers. Of course, when the degree of polymerization becomes very high, the perfect M state is entropically unfavorable, and the possibility of the imperfect helical state containing the helix reversals increases.

Cooperativity in the conformation of helical polymers mentioned above can be formulated using the Ising model which was originally proposed to deal with the order-disorder transition in ferromagnetic materials.²¹ In the above discussion, we have simply considered the energies of the P and M states as well as of the helix reversal. However, those states are also entropically different. In what follows, the difference in the free energy between the P and M states per monomer unit is denoted as $2\Delta G_h$, and the free energy of the helical reversal is denoted as ΔG_r , where the middle point of the free energies of the P and M states is taken as zero of the free energy. According to the theory of Lifson et al. based on

Ising model,¹⁸ the fraction f_M of the M state of the helical polymer in the solution (or the enantiomer excess of the right handed state, $2f_M-1$) can be calculated from ΔG_h , ΔG_r , the degree of polymerization N , and the absolute temperature T . (The original theory of Lifson et al. did not include the entropic difference of the helical states.²²)

The discrimination ΔG_h of the P and M states can be introduced by various methods. The chemical introduction of optically active side chains into a helical polymer is the most popular method for the discrimination. The physical interaction of a helical polymer chain with chiral solvent or neighboring chiral polymer chains in solution is another method for the discrimination. As explained above, a small ΔG_h is enough to discriminate the polymer helical conformation due to the cooperativity.

Cooperativity is also reflected on helicity of chiral-achiral and *RS* random copolymers. Figure 1-3 shows examples of the cooperativity in the chiral-achiral and *RS* random copolyisocyanates. In Panel A, the copolymerization of a small amount of the chiral monomer in PI 1 induces a sharp increase in the optical rotation of the polyisocyanate chain.²³ This type of chiral-achiral random copolymer is often called as the "sergeants-and-soldiers" copolymer, because achiral monomer units (soldiers) obey the preferred sense of the minor chiral monomer units (sergeants). On the other hand, the chiral-achiral random copolyisocyanate PI-2 in Panel A exhibits a helical sense inversion with changing the chiral

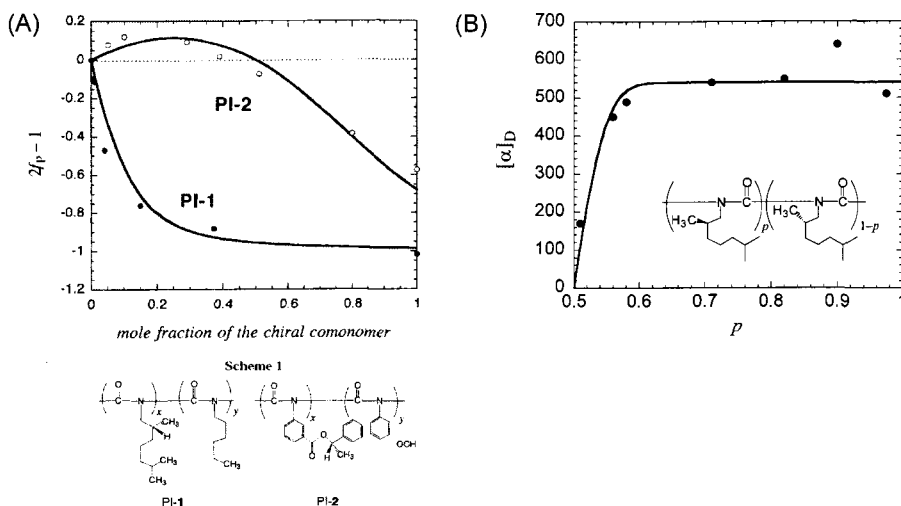


Figure 1-3. Composition dependences of the enantiomer excess for “sergeants-and-soldiers” polyisocyanates (A), and of the optical rotation of a “majority-rule” polyisocyanate (B).

monomer content. That is, in this copolyisocyanate the achiral monomer unit does not obey the order of the chiral monomer unit. A nonlinear phenomenon is also observed in *RS* random copolymers, as shown in Panel B of Figure 1-3.²¹ An abrupt transition from almost perfectly right- to left-handed helices occurs by a small change of the monomer content from the racemic state. These helical copolymers are referred to as the “majority-rule copolymer.”

There are helical polymers reported that the introduction of optically active side chains did not induce CD in dilute solution. Some of them, however, induce CD after the phase separation or aggregation take place in their solutions by addition of non-solvent or reducing temperature.

Optically active polythiophene and polysilane derivatives are famous examples.^{24,25} In these aggregation- and phase-separation-induced CD, the intermolecular chiral interaction among helical polymer chains may play an important role. However, the detailed mechanism of these phenomena has not been elucidated yet.

1.4 Study of Polyfluorenes

Polyfluorene is one of π -conjugated polymers. Polyfluorene itself is hardly dissolved in common solvents, but substitution of side chains increases its solubility to organic solvents as well as water and reduces its crystallinity.²⁶ Polyfluorene derivatives have interesting electrical and optical properties and attract increasing interest as a candidate for organic light-emitting diodes with high quantum yield and high hole mobility.

Figure 1-4 shows the molecular structure of polyfluorene derivatives. In the backbone, only the internal rotation around the bond \mathbf{b}_2 is permitted. However, the internal rotation is not free. On one hand, π -orbitals of the carbon atoms connected by the bond \mathbf{b}_2 tend to overlap to gain the π -bonding energy, which makes the polyfluorene backbone planer. On the other hand, the perfectly planer conformation slightly increases the conformational energy due to the steric repulsion between hydrogen atoms indicated by circles in Figure 1-4. As the result, the polyfluorene chain tends to take a tilted conformation.²⁷

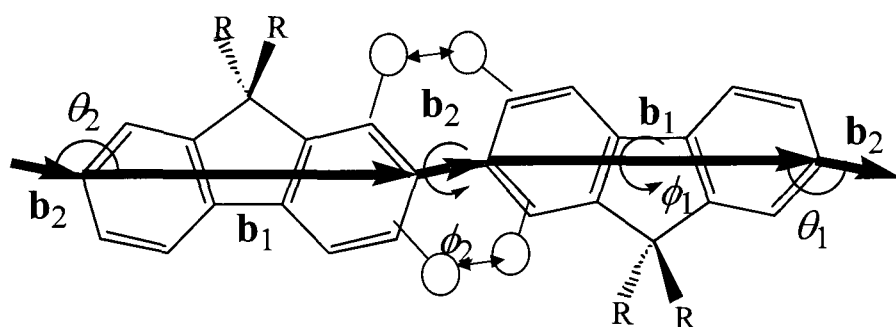


Figure 1-4. Molecular structure of a polyfluorene derivative.

Molecular modeling based on *ab initio* molecular orbital calculations indicated that the energetically favorable conformation of the polyfluorene backbone is 5/2 or 5/1 helix with taking the internal rotation angle ϕ_2 (cf. Figure 1-4) = 143° and 68° ,²⁸ respectively, and the former helical conformation was confirmed by electron and X-ray diffraction from spin-coated film and fiber of a polyfluorene derivative as well as from a solution study. The stable conformation of polyfluorene derivatives in the solid state is however dependent on the side chain R substituted. The 5/2 helix was observed for polyfluorene with branched alkyl side chains, poly(9,9-bis(2-ethylhexyl)fluorene), and the chain is packed hexagonally in crystal. On the other hand, polyfluorene with linear alkyl side chains, e.g., poly(9,9-di-*n*-octylfluorene), often takes a more planer conformation, called sometimes as the " β -phase" with $\phi_2 \approx 160^\circ$, and side chains of neighboring polyfluorene chains interpenetrate each other in crystal.²⁹

If optically active side chains are substituted to polyfluorene, we

might expect a helical conformation with a preferred handedness. Wu et al. reported that two optically active polyfluorenes shown in Figure 1-5 did not exhibit CD in dilute solution.³⁰ This may be owing to that the asymmetric carbon on the side chain is too far from the bond \mathbf{b}_2 to interact chirally.

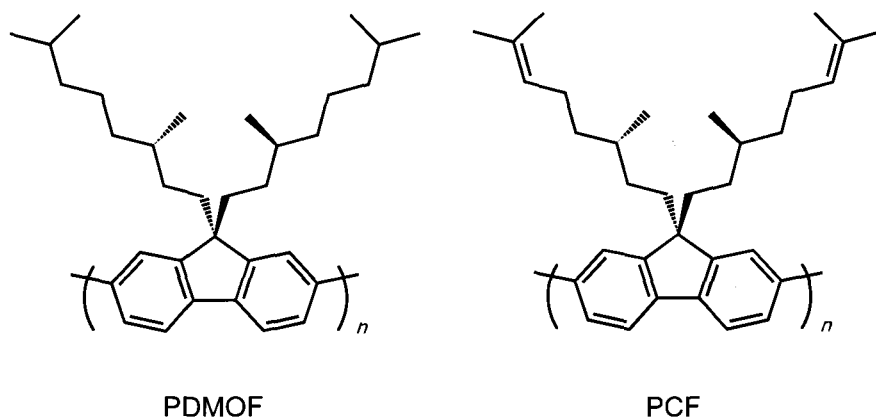


Figure 1-5. Chemical structures of two optically active polyfluorene derivatives studied by Wu et al.³⁰

Wu and Sato³⁰ found an exciton-coupling type CD at the wavelength of the backbone absorption in dilute tetrahydrofuran (THF) and toluene solutions upon cooling as low as -80 °C, where polyfluorene chains probably form aggregates. Oda et al. observed strong CD and circularly polarized electroluminescence for spin-coated films of some polyfluorenes bearing chiral alkyl side chains after annealing. These results indicate that the chiral discrimination is induced by an intermolecular chiral interaction among optically active polyfluorene chains in condensed systems so that

the polyfluorene backbone takes a preferred helical sense.

1.5 Purpose of This Study

Although Wu and Sato³⁰ found the aggregation induced CD for optically active polyfluorenes at ca. $-80\text{ }^{\circ}\text{C}$, characterization of polyfluorene aggregates in solution at $-80\text{ }^{\circ}\text{C}$ was rather difficult, so that detailed mechanism of the aggregation-induced CD was not investigated.

In this study, we have searched the solvent condition where an optically active polyfluorene derivative exhibits CD in dilute solution near the room temperature. Poly(2,7-[9,9-bis((*S*)-citronellyl)]fluorene) (PCF, cf. Figure 1-5) was chosen as the test polymer, and the phase-separation induced CD was found in dilute THF solutions of this polymer near the room temperature, by adding a non-solvent, methanol. To elucidate detailed mechanism of the phase-separation-induced CD, we have investigated the kinetics of CD induced upon cooling the THF-methanol solution, as well as the phase-separating solutions by light scattering measurements. The latter measurements provided us information about the CD active concentrated phase in the phase-separating solution. On the basis of those experimental results, we have proposed a model for the CD induction in phase-separating solutions of helical polymers. This study on the phase-separation induced CD phenomenon in PFC is described in Chapter 2.

As mentioned in Section 1.3, helical chiral-achiral random copolymers

often exhibit interesting chiroptical properties, e.g., sergeants-and-soldiers behavior, the composition-driven helical screw-sense inversion,^{31,32} and so on. Therefore, it may be interesting to extend the CD induction study in phase separating solution to a helical chiral-achiral random copolyfluorene. In this study, a random copolymer, poly(2,7-[9,9-bis((*S*)-citronellyl)]fluorene-*random*-9,9-di-*n*-octyl fluorene) shown in Figure 1-6 was chosen to study the phase separation induced CD, and a double screw-sense inversions by changing the chiral monomer content x was found. The results are presented in Chapter 2.

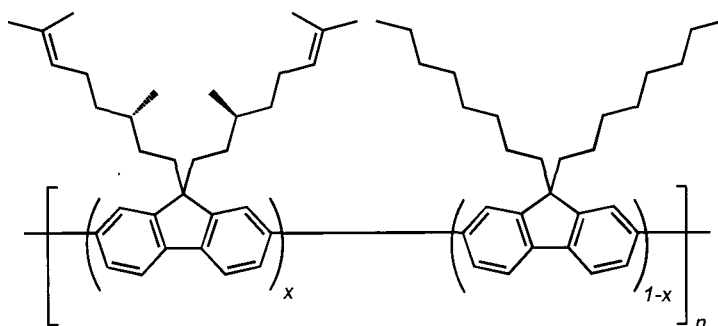


Figure 1-6. Chemical structure of a chiral-achiral copolymer of optically active/inactive fluorene derivative.

As will be explained in Chapters 2 and 3, the phase separation CD induction mentioned above was concluded to occur by nonracemization of helical state of the main chain of optically active polyfluorene due to the

intermolecular chiral interaction in the phase separated concentrated phase. To clarify the packing structure of polyfluorene chains in the concentrated phase, we carried out X-ray scattering measurements on non-phase separated concentrated solutions of polyfluorene. THF used for the CD induction experiment is a volatile solvent not being suitable for measurements of concentrated solutions. Therefore we chose mesitylene as another good solvent. The results of X-ray scattering measurements are shown in Chapter 4.

Summary of main results and conclusions obtained in this work are given in Chapter 5.

1.6 References

- 1 Ziegler, K., Holzkamp, E., Breil, H. & Martin, H. Das Mülheimer Normaldruck-Polyäthylen-Verfahren. *Angewandte Chemie* **67**, 541-547 (1955).
- 2 Natta, G. Stereospecific polymerizations by means of coordinated anionic catalysis: Introductory Lecture. *Journal of Inorganic and Nuclear Chemistry* **8**, 589-611 (1958).
- 3 Ito, T., Shirakawa, H. & Ikeda, S. Simultaneous polymerization and formation of polyacetylene film on the surface of concentrated soluble Ziegler-type catalyst solution. *Journal of Polymer Science: Polymer Chemistry Edition* **12**, 11-20 (1974).

- 4 Shirakawa, H., Louis, E. J., MacDiarmid, A. G., Chiang, C. K. & Heeger, A. J. Synthesis of electrically conducting organic polymers: halogen derivatives of polyacetylene, (CH). *Journal of the Chemical Society, Chemical Communications*, 578-580 (1977).
- 5 Heeger, A. J., Kivelson, S., Schrieffer, J. R. & Su, W. P. Solitons in conducting polymers. *Reviews of Modern Physics* **60**, 781 (1988).
- 6 Miyaura, N., Yamada, K. & Suzuki, A. A new stereospecific cross-coupling by the palladium-catalyzed reaction of 1-alkenylboranes with 1-alkenyl or 1-alkynyl halides. *Tetrahedron Letters* **20**, 3437-3440 (1979).
- 7 Rault-Berthelot, J. & Simonet, J. The anodic oxidation of fluorene and some of its derivatives: Conditions for the formation of a new conducting polymer. *Journal of Electroanalytical Chemistry and Interfacial Electrochemistry* **182**, 187-192 (1985).
- 8 Heck, R. F. & Nolley, J. P. Palladium-catalyzed vinylic hydrogen substitution reactions with aryl, benzyl, and styryl halides. *The Journal of Organic Chemistry* **37**, 2320-2322 (1972).
- 9 Tamao, K., Sumitani, K. & Kumada, M. Selective carbon-carbon bond formation by cross-coupling of Grignard reagents with organic halides. Catalysis by nickel-phosphine complexes. *Journal of the American Chemical Society* **94**, 4374-4376 (1972).
- 10 Yamamoto, T., Ito, T. & Kubota, K. A Soluble Poly(arylene) with

- Large Degree of Depolarization. Poly(2,5-pyridinediyl) Prepared by Dehalogenation Polycondensation of 2,5-Dibromopyridine with Ni(0)-Complexes. *Chemistry Letters* **17**, 153-154 (1988).
- 11 Pope, M., Kallmann, H. P. & Magnante, P. Electroluminescence in Organic Crystals. *The Journal of Chemical Physics* **38**, 2042-2043 (1963).
 - 12 Garnier, F., Hajlaoui, R., Yassar, A. & Srivastava, P. All-Polymer Field-Effect Transistor Realized by Printing Techniques. *Science* **265**, 1684-1686 (1994).
 - 13 Yu, G., Gao, J., Hummelen, J. C., Wudl, F. & Heeger, A. J. Polymer Photovoltaic Cells: Enhanced Efficiencies via a Network of Internal Donor-Acceptor Heterojunctions. *Science* **270**, 1789-1791 (1995).
 - 14 Burroughes, J. H., Bradley, D. D. C., Brown, A. R., Marks, R. N., Mackay, K., Friend, R. H., Burns, P. L. & Holmes, A. B. Light-emitting diodes based on conjugated polymers. *Nature* **347**, 539-541 (1990).
 - 15 Gustafsson, G., Cao, Y., Treacy, G. M., Klavetter, F., Colaneri, N. & Heeger, A. J. Flexible light-emitting diodes made from soluble conducting polymers *Nature* **357**, 477-479 (1992).
 - 16 Gustafsson, G., Treacy, G. M., Cao, Y., Klavetter, F., Colaneri, N. & Heeger, A. J. The "plastic" led: A flexible light-emitting device using a polyaniline transparent electrode. *Synthetic Metals* **57**, 4123-4127

- (1993).
- 17 Brown, A. R., Greenham, N. C., Burroughes, J. H., Bradley, D. D. C., Friend, R. H., Burn, P. L., Kraft, A. & Holmes, A. B. Electroluminescence from multilayer conjugated polymer devices: Spatial control of exciton formation and emission. *Chemical Physics Letters* **200**, 46-54 (1992).
 - 18 Green, M. M., Peterson, N. C., Sato, T., Teramoto, A., Cook, R. & Lifson, S. A Helical Polymer with a Cooperative Response to Chiral Information. *Science* **268**, 1860-1866 (1995).
 - 19 Wu, Z.-Q., Nagai, K., Banno, M., Okoshi, K., Onitsuka, K. & Yashima, E. Enantiomer-Selective and Helix-Sense-Selective Living Block Copolymerization of Isocyanide Enantiomers Initiated by Single-Handed Helical Poly(phenyl isocyanide)s. *Journal of the American Chemical Society* **131**, 6708-6718 (2009).
 - 20 Bredas, J. L., Adant, C., Tackx, P., Persoons, A. & Pierce, B. M. Third-Order Nonlinear Optical Response in Organic Materials: Theoretical and Experimental Aspects. *Chemical Reviews* **94**, 243-278 (1994).
 - 21 Gu, H., Nakamura, Y., Sato, T., Teramoto, A., Green, M. M., Jha, S. K., Andreola, C. & Reidy, M. P. Optical Rotation of Random Copolyisocyanates of Chiral and Achiral Monomers: Sergeant and Soldier Copolymers†. *Macromolecules* **31**, 6362-6368 (1998).

- 22 Lifson, S., Green, M. M., Andreola, C. & Peterson, N. C. Macromolecular stereochemistry: helical sense preference in optically active polyisocyanates. Amplification of a conformational equilibrium deuterium isotope effect. *Journal of the American Chemical Society* **111**, 8850-8858 (1989).
- 23 Sato, T., Terao, K., Teramoto, A. & Fujiki, M. On the Composition-Driven Helical Screw-Sense Inversion of Chiral-Achiral Random Copolymers. *Macromolecules* **35**, 5355-5357 (2002).
- 24 Zhang, Z.-B., Fujiki, M., Motonaga, M., Nakashima, H., Torimitsu, K. & Tang, H.-Z. Chiroptical Properties of Poly{3,4-bis[(S)-2-methyloctyl]thiophene}. *Macromolecules* **35**, 941-944 (2001).
- 25 Nakashima, H., Fujiki, M. & Koe, J. R. Helical Poly(alkylalkoxyphenylsilane)s Bearing Enantiopure Chiral Groups on the Phenyl Rings. *Macromolecules* **32**, 7707-7709 (1999).
- 26 Liu, B., Yu, W.-L., Lai, Y.-H. & Huang, W. Blue-Light-Emitting Cationic Water-Soluble Polyfluorene Derivatives with Tunable Quaternization Degree. *Macromolecules* **35**, 4975-4982 (2002).
- 27 Wu, L., Sato, T., Tang, H.-Z. & Fujiki, M. Conformation of a Polyfluorene Derivative in Solution. *Macromolecules* **37**, 6183-6188 (2004).

- 28 Hong, S. Y., Kim, D. Y., Kim, C. Y. & Hoffmann, R. Origin of the Broken Conjugation in m-Phenylene Linked Conjugated Polymers. *Macromolecules* **34**, 6474-6481 (2001).
- 29 Chunwaschirasiri, W., Tanto, B., Huber, D. L. & Winokur, M. J. Chain Conformations and Photoluminescence of Poly(di-n-octylfluorene). *Physical Review Letters* **94**, 107402 (2005).
- 30 Wu, L. & Sato, T. Aggregation-Induced Circular Dichroism of Optically Active Polyfluorene Derivatives in Solution. *KOBUNSHI RONBUNSHU* **63**, 505-511 (2006).
- 31 Maeda, K. & Okamoto, Y. Synthesis and Conformational Characteristics of Poly(phenyl isocyanate)s Bearing an Optically Active Ester Group. *Macromolecules* **32**, 974-980 (1999).
- 32 Koe, J. R., Fujiki, M., Motonaga, M. & Nakashima, H. Cooperative Helical Order in Optically Active Poly(diarylsilylenes). *Macromolecules* **34**, 1082-1089 (2001).

Chapter 2.

Phase-Separation Induced Circular Dichroism in Dilute Solutions of an Optically Active Polyfluorene Homopolymer

2.1 Introduction

Polyfluorene, a π -conjugated polymer, has interesting electrical and optical properties and attracts increasing interest as a candidate for organic light-emitting diodes with high quantum yield and high hole mobility.^{1, 2} Circular dichroism (CD), optical activity, and circular polarized luminescence are additional optical and electro-optical properties that enable polyfluorene to be utilized in optical devices or sensors. Several researchers³⁻⁷ were interested in these properties and investigated optically active polyfluorene derivatives bearing chiral side chains.

Molecular modeling based on *ab initio* molecular orbital calculations indicated that the energetically favorable conformation of the polyfluorene backbone is a 5/2 or 5/1 helix,^{8, 9} and this helical conformation was supported by electron and X-ray diffraction from the spin-coated film and fiber of a polyfluorene derivative^{8, 10}, as well as from a solution study.⁶ However, dilute solutions of optically active polyfluorene derivatives usually exhibit little CD.^{6, 7} This implies that the optically active side chain hardly differentiates the energies of the right- and left-handed helical conformations of the polyfluorene backbone. On the other hand, strong CD,

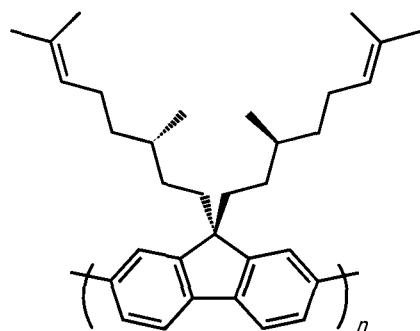
circular selective reflection, and circular polarized luminescence were observed for optically active polyfluorene derivative films, demonstrating that the chiral discrimination arises from the intermolecular interaction in the condensed phase.^{3, 4, 11}

Some π - and σ -conjugated polymers, e.g., polythiophene and polysilane derivatives, were reported to induce strong CD in dilute solutions by aggregation or phase separation.¹²⁻¹⁵ In these aggregation- and phase-separation-induced CD, the intermolecular chiral interaction among conjugated polymer chains may play an important role. However, the detailed mechanism of these phenomena has not been elucidated.

Recently, Wu and Sato⁷ reported aggregation-induced CD in dilute tetrahydrofuran (THF) and toluene solutions of two optically active polyfluorene derivatives upon cooling to as low as -80 °C. The observed exciton-coupling signal of CD arising from the polyfluorene main-chain was inverted by changing the solvents (THF and toluene) or through tiny differences in the side-chain chemical structure. Because of the difficulty in characterization of polyfluorene aggregates in solution at -80 °C, the detailed mechanism of the aggregation- induced CD was not investigated in the previous study.

In this study, we have investigated the solvent condition where an optically active polyfluorene derivative exhibits CD in a dilute solution near room temperature. Poly(2,7-[9,9-bis((*S*)-citronellyl)]fluorene) (PCF,

Scheme 2-1) was chosen as the test polymer, and phase-separation induced CD was found in dilute THF solutions of this polymer near room temperature by adding a non-solvent, methanol. To elucidate the detailed mechanism of the CD induction, we have investigated the kinetics of CD induced upon cooling in the THF-methanol solution, as well as the separated droplet phase, by light scattering measurements. On the basis of those experimental results, we have proposed a model for CD induction in phase-separating solutions of helical polymers.



Scheme 2-1. Repeating unit of PCF.

2.2 Experimental Section

2.2.1 Polymer Samples

The dibromofluorene monomer was polymerized in a hot mixture of toluene and *N,N*-dimethylformamide (DMF) using a zero-valent nickel

reagent by the Yamamoto coupling reaction.⁵ The polymer was divided into 7 fractions by fractional precipitation using toluene as the solvent and methanol as the precipitant. Two fractions, PCF2-1 and PCF2-3, were chosen for the following experiments. The solvents THF and methanol were distilled under calcium hydrate as a desiccant.

2.2.2 Turbidity

Methanol was added dropwise under stirring to THF solutions of the fraction PCF2-1 with different polymer concentrations, and the turbidity of each solution was observed at room temperature by eye to construct the ternary phase diagram of PCF, THF, and methanol. In what follows, the composition of the ternary system is expressed in terms of the volume fraction ϕ_{MeOH} of methanol at the mixing of THF and methanol and the PCF mass concentration c in the total solution.

2.2.3 Circular Dichroism and UV-VIS Absorption

Circular dichroism (CD) and ultraviolet-visible light (UV-VIS) absorption spectra were measured on phase-separating solutions of fraction PCF2-1 with $\phi_{\text{MeOH}} = 0.5$ and different c using a JASCO J-720WO spectropolarimeter at 40 °C and 15 °C. A quartz cell with a 10-cm optical pass length and a thermostat jacket was used for the measurements.

2.2.4 Light Scattering

Static light scattering measurements were carried out on THF and methanol-added THF solutions of samples PCF2-1 and PCF2-3 using a Fica 50 light scattering photometer with vertically polarized incident light of 546 nm and without an analyzer. The light scattering systems were calibrated using toluene as the reference material.

For THF solutions of the two PCF samples, the Rayleigh ratio R_θ excess over that of the solvent obtained at the scattering angle θ was analyzed by the conventional Berry plot to determine the weight-average molar mass M_w , the second virial coefficient A_2 , and the z-average square radius of gyration $\langle S^2 \rangle$ using the equations¹⁶

$$\lim_{\theta \rightarrow 0} \left(\frac{Kc}{R_\theta} \right)^{1/2} = \frac{1}{M_w^{1/2}} + A_2 M_w^{1/2} c + \dots, \quad \lim_{c \rightarrow 0} \left(\frac{Kc}{R_\theta} \right)^{1/2} = \frac{1}{M_w^{1/2}} \left(1 + \frac{1}{6} \langle S^2 \rangle k^2 + \dots \right) \quad (1)$$

where K is the optical constant defined by $K = 4\pi^2 n_0 (\partial n / \partial c)^2 / N_A \lambda^4$ with the solvent refractive index n_0 , the specific refractive index increment $\partial n / \partial c$, the Avogadro constant N_A , and the wavelength of the incident light *in vacuo* λ , and k is the magnitude of the scattering vector defined by $k = (4\pi n_0 / \lambda) \sin(\theta/2)$. The results of M_w , A_2 , and $\langle S^2 \rangle^{1/2}$ for samples PCF2-1 and PCF2-3 in THF are listed in Table 2-I.

Table 2-I. Molecular characteristics of the PFC samples used.

sample	$M_w/10^5$	$A_2/10^{-3}\text{cm}^3\text{molg}^{-2}$	$\langle S^2 \rangle^{1/2}/\text{nm}$
PCF2-1	1.21	1.32	35.3
PCF2-3	1.29	1.38	31.6

Light scattering from the polymer in a mixed solvent is affected by preferential adsorption. Due to this effect, eq. 1 should be replaced by the following equation,¹⁷

$$\lim_{c \rightarrow 0} \left(\frac{Kc}{R_\theta} \right)^{1/2} \left[1 + \left(\frac{\partial c_1}{\partial c_2} \right)_{\mu_1} \frac{(\partial \tilde{n} / \partial c_1)_{c_2}}{(\partial \tilde{n} / \partial c_2)_{c_1}} \right] \equiv \lim_{c \rightarrow 0} \left(\frac{K^*c}{R_\theta} \right)^{1/2} = \frac{1}{M_w^{1/2}} \left(1 + \frac{1}{6} \langle S^2 \rangle k^2 + \dots \right) \quad (2)$$

where $(\partial c_1 / \partial c)_{\mu_1}$ is the increment of the mass concentration c_1 of the secondary solvent (methanol in our system) with increasing c at a constant solvent chemical potential, and $(\partial \tilde{n} / \partial c)_{c_1}$ and $(\partial \tilde{n} / \partial c)_{c_2}$ are the specific refractive index increments of the polymer and the secondary solvent components, respectively.

The specific refractive index increment $(\partial\tilde{n}/\partial c)_{c_1}$ at constant solvent composition, included in K , was measured at 30 °C using a differential refractometer of the modified Schulz-Cantow type. Figure 2-1 shows the results of $(\partial\tilde{n}/\partial c)_{c_1}$ at $\phi_{\text{MeOH}}(c_1) = 0$ (0 g/cm³), 0.2 (0.21 g/cm³), and 0.35 (0.38 g/cm³), represented by filled circles. The value of $(\partial\tilde{n}/\partial c)_{c_1}$ at $\phi_{\text{MeOH}}(c_1) = 0.5$ (0.57 g/cm³) was obtained by extrapolation (unfilled circle in Figure 2-1).

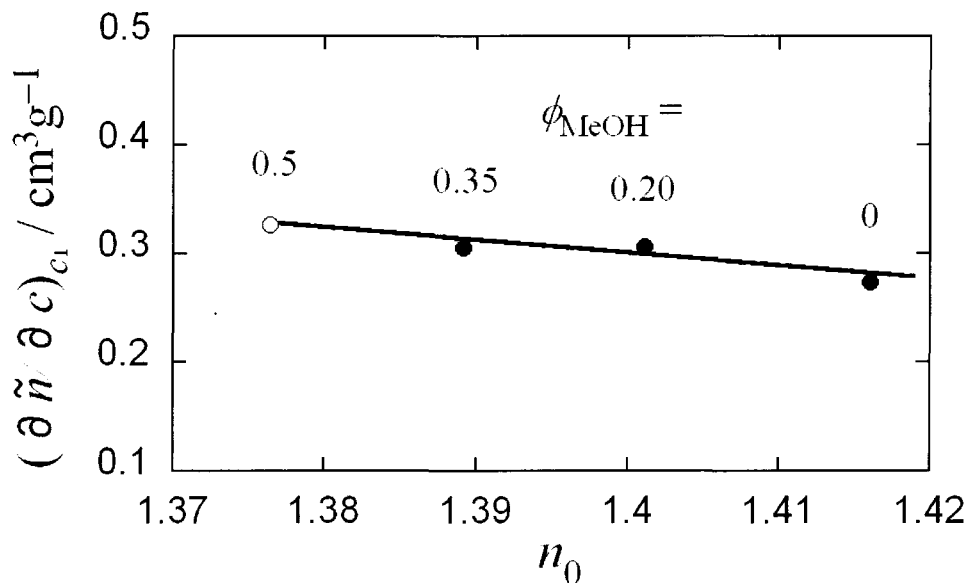


Figure 2-1. Specific refractive index increments of PCF in THF and HF-methanol mixtures at 30 °C.

2.3 Results and Discussion

2.3.1 Phase Diagram

Figure 2-2 illustrates the phase diagram of the ternary system of sample PCF2-1, THF, and methanol at room temperature. Here c is the polymer mass concentration, ϕ_{MeOH} is the volume fraction of methanol at the mixing of THF and methanol, and the unfilled and filled circles indicate single-phase and biphasic states, respectively. This is a typical ternary phase diagram of a polymer, solvent, and non-solvent.¹⁸ CD and UV-VIS

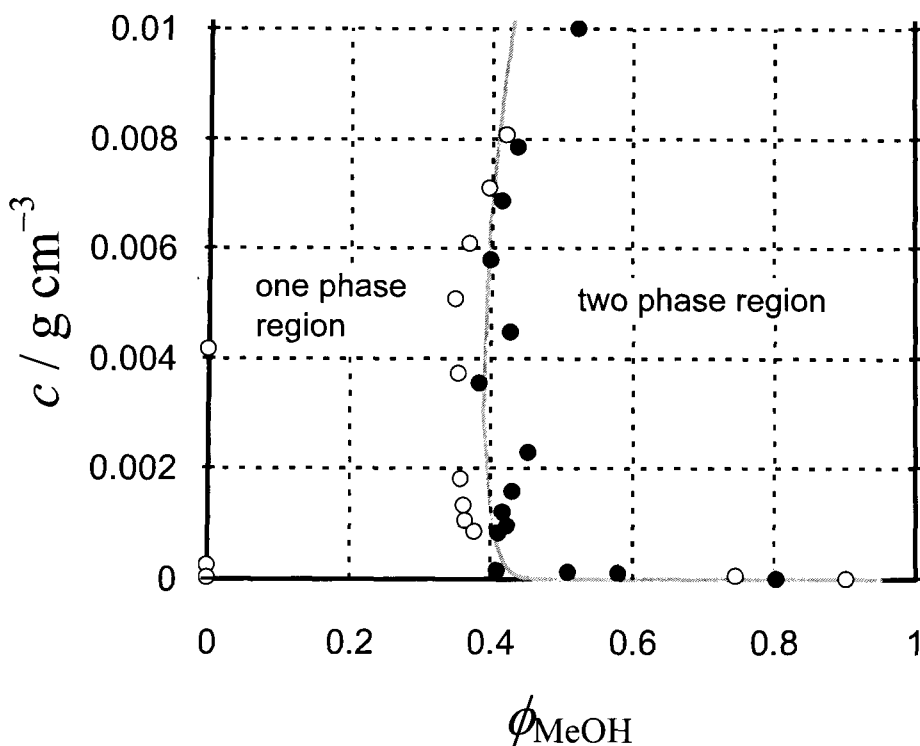


Figure 2-2. Phase diagram of the ternary system PCF, THF, and methanol at room temperature; unfilled circles, one-phase region; filled circles, two-phase region.

absorption as well as light scattering measurements, mentioned below, were made in the two-phase region mostly at fixed $\phi_{\text{MeOH}} = 0.5$.

2.3.2 Circular Dichroism and UV-VIS Absorption

Figure 2-3 shows CD and UV-VIS absorption spectra of sample PCF2-1 in the THF-methanol mixture of $\phi_{\text{MeOH}} = 0.5$ ($c = 6.0 \times 10^{-7} \text{ g/cm}^3$). Although the solution is CD inactive at 40 °C, a bisign signal grows upon cooling of the solution to 15 °C. While the peak height of the UV-VIS absorption decreases with the cooling time, that of the CD spectrum increases, except at 300 min. The diminishment of the absorption spectrum may arise from the increase of scattering from the solution; the scattered light cannot contribute to the absorption. (Although not shown, the baseline of the original UV-VIS absorption curve was considerably dependent on the wavelength λ according to Rayleigh's λ^{-4} -law¹⁶ and increased with time at 15 °C. This baseline was subtracted from the original absorption curve to obtain A , shown in Figure 2-3.) Similar CD and UV-VIS absorption spectra were obtained at different c ($= 2.0 \times 10^{-7} \text{ g/cm}^3$ and $4.0 \times 10^{-7} \text{ g/cm}^3$). These CD inductions were almost reversible, that is, when the quenched solutions were heated to 40 °C, the induced CD vanished again.

In Figure 2-3, the UV-VIS absorption peak seems to show a slight red shift. If this red shift reflects the transformation to the β -phase of

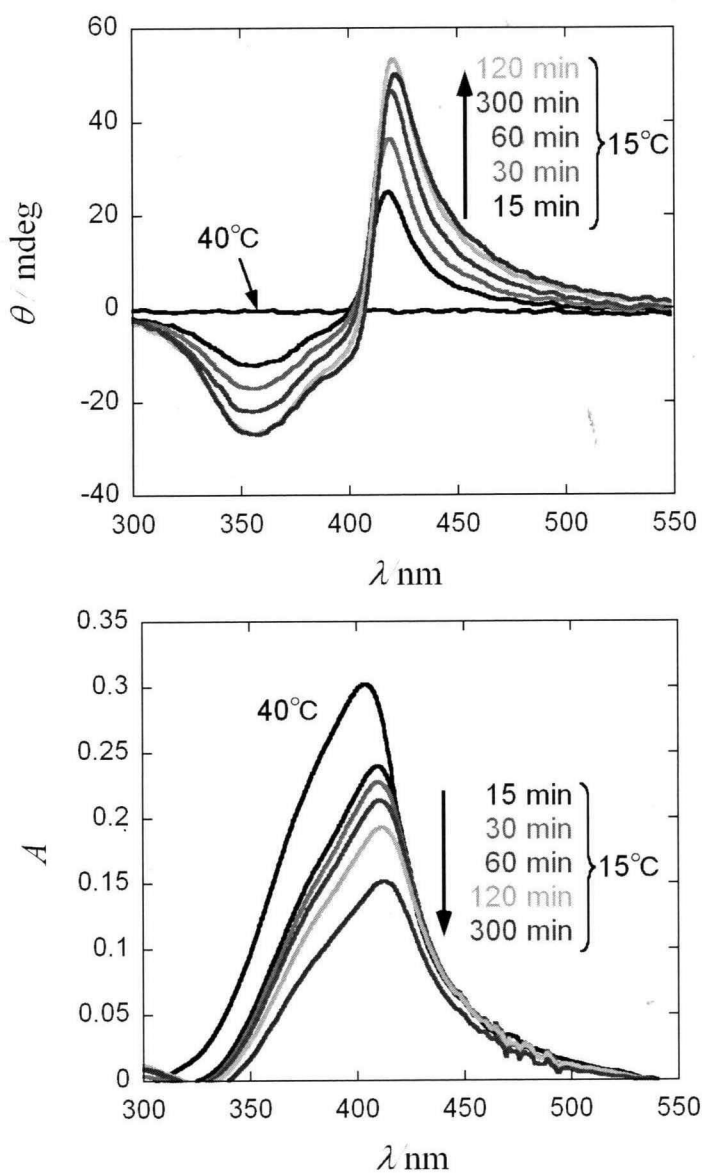


Figure 2-3. CD and UV-VIS absorption spectra for a phase-separating solution of sample PCF2-1 ($\phi_{\text{MeOH}} = 0.5$, $c = 6.0 \times 10^{-7} \text{ g/cm}^3$) at 40°C and quenched to 15°C .

polyfluorene chains,¹⁹ the peak should return to the original position upon heating to 40 °C. However, the red shift was not reversible. The UV-VIS absorption experiment for the phase-separating solutions is affected by the wavelength-dependent scattering, and the baseline subtraction may not be enough to perfectly correct this scattering effect. Owing to this experimental uncertainty, we do not argue the origin of the small peak shift here.

The induced CD must arise from the separating concentrated phase, and the molar circular dichroism $\Delta\varepsilon_c$ of the concentrated phase is calculated from the observed ellipticity θ by

$$\Delta\varepsilon_c = \frac{4\pi \log e}{180} \frac{\theta}{(1000c_c/M_0)\Phi l} \quad (3)$$

where c_c and Φ are the mass concentration and the volume fraction (in the total solution) of the concentrated phase, respectively, M_0 is the molar mass of the PCF repeating unit, and l is the path length; Φl represents the average path length of the concentrated phase. On the other hand, the average molar extinction coefficient ε_c of the concentrated phase is calculated from the observed absorbance A using

$$\varepsilon_c = \frac{A(c - c_d)/c}{(1000c_c/M_0)\Phi l} \quad (4)$$

where c_d is the mass concentration of the coexisting dilute phase. Thus, the Kuhn dissymmetry factor of the concentrated phase may be proportional to

the following quantity:²⁰

$$g_c \equiv \Delta\epsilon_{c,m}/\epsilon_{c,m} = \frac{4\pi \log e}{180} \frac{\theta_m}{A_m (c - c_d)/c}. \quad (5)$$

Here, θ_m and A_m are the peak heights of ellipticity and absorbance, respectively.

The value of c_d was estimated by light scattering (cf. Figure 2-6).

Figure 2-4 displays the time evolution of g_c of the solutions shown in Figure 2-3 after quenching from 40 to 15 °C. The data points can be fitted to single-exponential functions (solid curves in the figure), although the initial and final g_c values are slightly different at each polymer concentration c . Therefore, the CD induction obeys first-order reaction kinetics (cf. the discussion at the end of this section). From the fitting curves, the reaction rate constant was estimated to be $2.5 \times 10^{-4} \text{ s}^{-1}$. Thus, the CD induction is a rather slow molecular event.

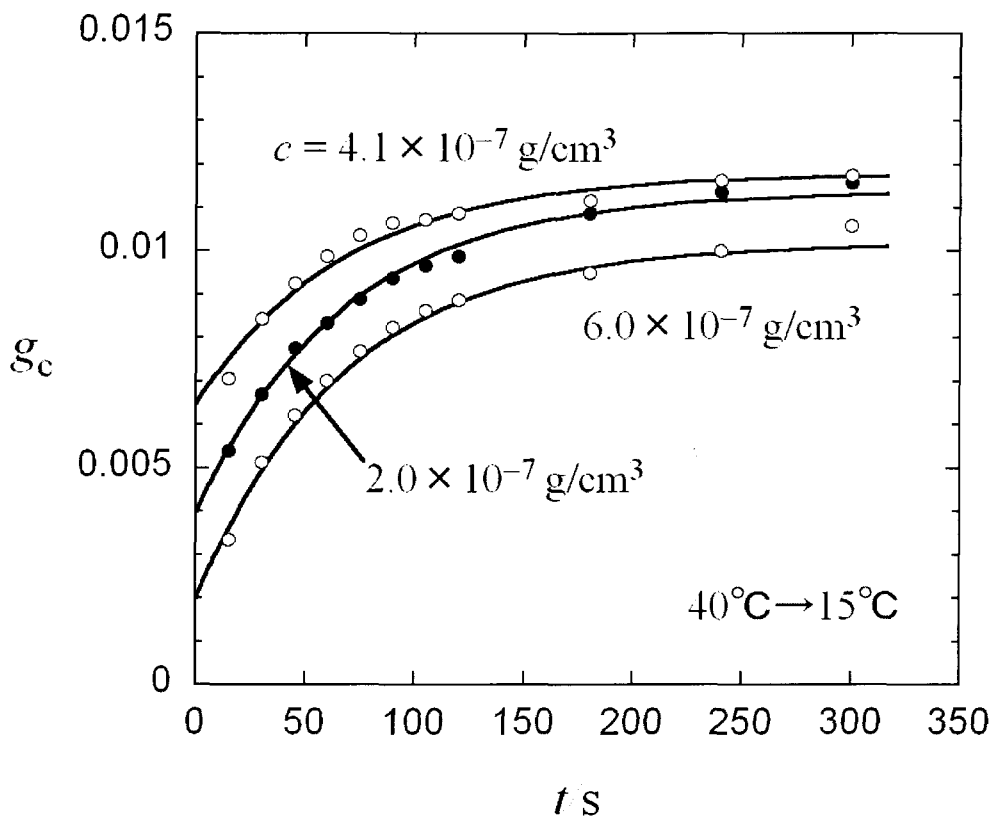


Figure 2-4. Time evolution of the Kuhn dissymmetry factor for the concentrated phase in the phase-separating solution shown in Figure 2-3 after quenched from 40 °C to 15 °C; solid curves, single-exponential fitting results (cf. eq 14)

2.3.3 Light Scattering

Figure 2-5 compares $(Kc/R_\theta)^{1/2}$ at $\theta \rightarrow 0$ for sample PCF2-3 in THF and a THF-methanol mixture with $\phi_{\text{MeOH}} = 0.2$. The disagreement of the intercepts comes from preferential adsorption, and using eq. 2 we can estimate the degree of preferential adsorption $(\partial c_1/\partial c)_{\mu_1}$ to be -0.025 . [At $\phi_{\text{MeOH}} = 0.2$, $(\partial \tilde{n}/\partial c_1)_{c=0} = -0.089 \text{ cm}^3/\text{g}$.] Neglecting the solvent composition dependence of $(\partial c_1/\partial c)_{\mu_1}$, we may calculate the optical constant K^* in eq. 2 at $\phi_{\text{MeOH}} = 0.5$ using $(\partial \tilde{n}/\partial c_1)_{c=0} = -0.11 \text{ cm}^3/\text{g}$ and

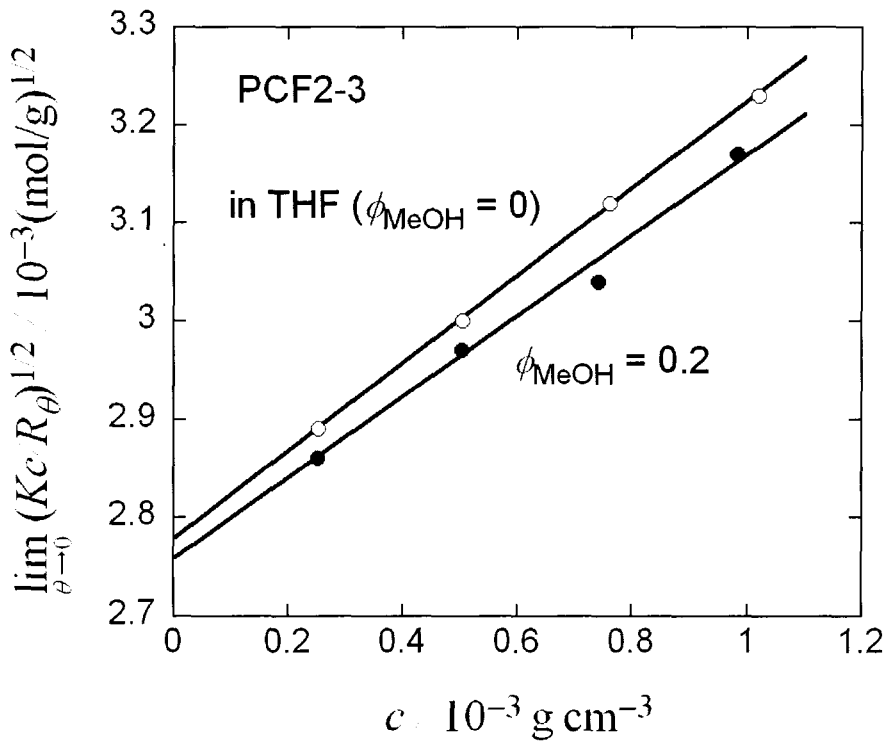


Figure 2-5. Concentration dependences of $(Kc/R_\theta)^{1/2}$ at $\theta \rightarrow 0$ for sample PCF2-3 in THF and a THF-methanol mixture with $\phi_{\text{MeOH}} = 0.2$.

$$(\partial \bar{n} / \partial c)_{c_1} = 0.326 \text{ cm}^3/\text{g} \text{ (cf. Figure 2-1).}$$

At $\phi_{\text{MeOH}} = 0.5$, R_θ is high enough, even for very dilute solutions, because droplets of the minor concentrated phase possess very strong scattering power. In Figure 2-6, $(R_\theta/K^*)^{1/2}$ at $\theta \rightarrow 0$ for sample PCF2-1 at $\phi_{\text{MeOH}} = 0.5$ and 40°C is plotted against c . From this plot, R_θ seems to vanish at ca. $3 \times 10^{-8} \text{ g/cm}^3$. This critical concentration can be regarded as the polymer concentration c_d of the coexisting dilute phase. In what follows, we are interested in droplets of the minor concentrated phase in the solution, which is responsible for the CD induction. The mass concentration of the concentrated phase droplets in the solution is given by $c - c_d$. Strictly

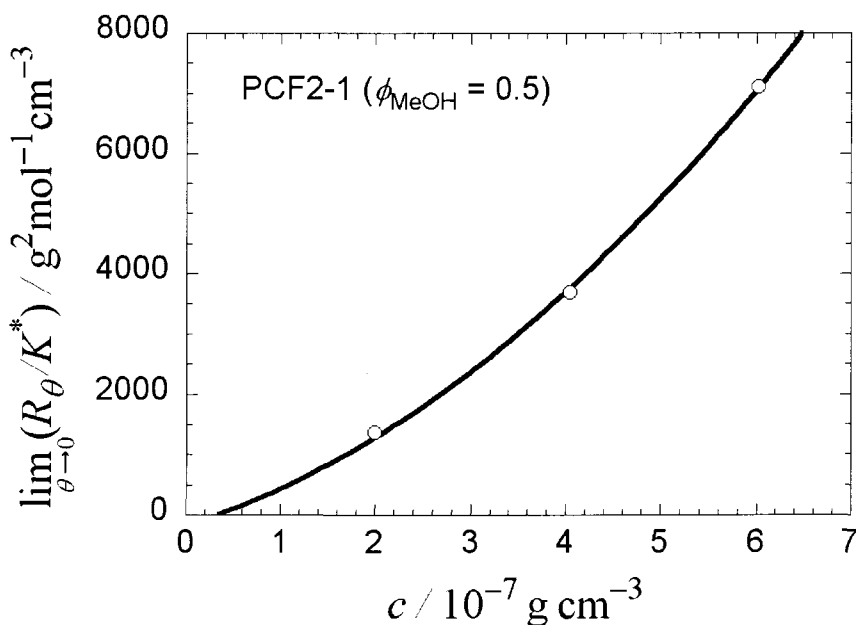


Figure 2-6. Concentration dependence of $(R_\theta/K^*)^{1/2}$ at $\theta \rightarrow 0$ for sample PCF2-1 at $\phi_{\text{MeOH}} = 0.5$ and 40°C .

speaking, c_d slightly depends on c , but within the dilute c range we examined c_d may be approximated to be $3 \times 10^{-8} \text{ g/cm}^3$, as determined in Figure 2-6, irrespective of c .

Figure 2-7 compares $[K^*(c - c_d)/R_\theta]^{1/2}$ for the concentrated droplet phase in a solution of sample PCF2-1 ($\phi_{\text{MeOH}} = 0.5, c = 6.0 \times 10^{-7} \text{ g/cm}^3$) at

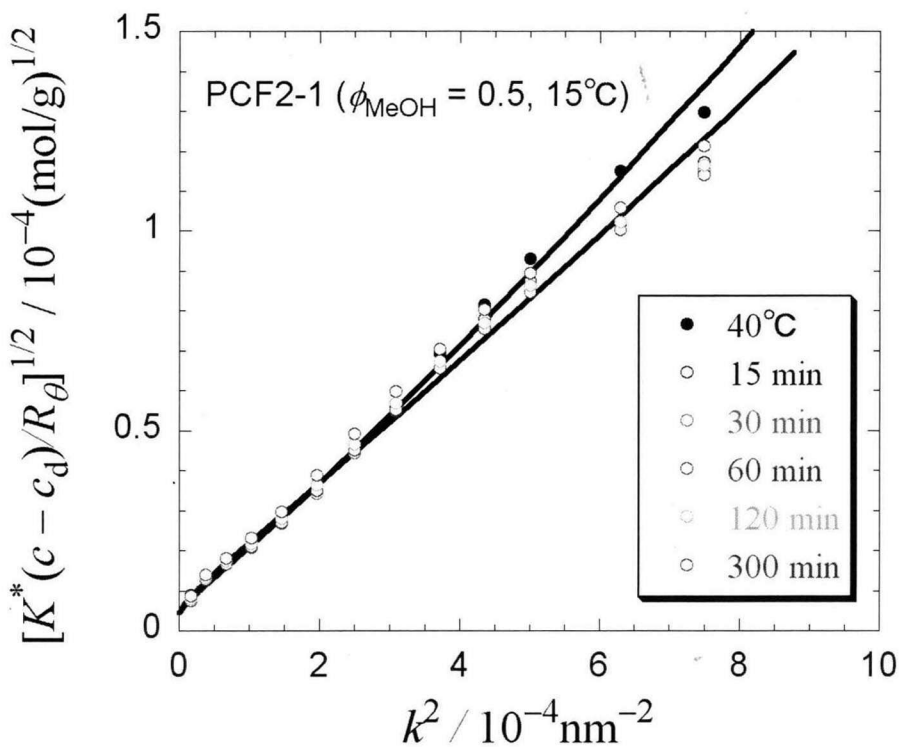


Figure 2-7. Angular dependences of $[K^*(c - c_d)/R_\theta]^{1/2}$ for the concentrated droplet phase in a solution of sample PCF2-1 ($\phi_{\text{MeOH}} = 0.5, c = 6.0 \times 10^{-7} \text{ g/cm}^3$) at 40 °C and upon cooling to 15 °C; solid curves, calculated by eqs 6-10 with the fitting parameters listed in Table 2-II.

40 °C and upon cooling to 15 °C. The scattering intensity and thus the size and amount of the droplet phase in the solution change little upon cooling. Similar temperature insensitive light scattering results were also obtained for solutions of sample PCF2-1 with $\phi_{\text{MeOH}} = 0.5$ and different c (2.0×10^{-7} g/cm³ and 4.1×10^{-7} g/cm³). This is in sharp contrast to the CD induction shown in Figure 2-3, indicating that the phase separation may be a necessary condition, but not a sufficient one, for CD induction.

Let us assume that the droplets of the concentrated phase are polydisperse spherical particles obeying a log-normal distribution. The log-normal distribution^{21, 22} is expressed in terms of the weight fraction $w(M)$ of the molar mass M given by

$$w(M) = \frac{1}{\sqrt{\pi}\beta M} \exp\left\{-\left[\beta^{-1} \ln(M/M^\circ)\right]^2\right\} \quad (6)$$

where

$$M^\circ = \sqrt{M_w M_n}, \quad \beta \equiv \sqrt{2 \ln(M_w/M_n)} \quad (7)$$

with weight- and number-average molar masses M_w and M_n . The particle scattering function $P(k)$ of the sphere with a molar mass M is given by²³

$$P(k) = \frac{9}{(kR)^6} [\sin(kR) - kR \cos(kR)]^2 \quad (8)$$

where R is the radius of the sphere related to M by

$$\frac{4\pi}{3} R^3 N_A c_c = M \quad (9)$$

with Avogadro's constant N_A and mass concentration c_c of the concentrated phase.

Polymer concentrations of the solutions investigated are so dilute ($< 10^{-6}$ g/cm³) that the interparticle interference effect may be neglected in the scattering intensity. In such a case, $K^*(c - c_d)/R_\theta$ can be calculated by^{16, 24}

$$\frac{K^*(c - c_d)}{R_\theta} = \frac{1}{M_w P_z(k)} = \left[\int_0^\infty MP(k)w(M)dM \right]^{-1}. \quad (10)$$

Figure 2-8 shows fitting results of $K^*(c - c_d)/R_\theta$ for phase-separating solutions of sample PCF2-1 with $\phi_{MeOH} = 0.5$ and three different c at 40 °C. The solid curves, drawn using eqs. 6 – 10 with the fitting parameters listed in Table 2-II, almost fit to the experimental data points. The weight-average molar mass M_w of the concentrated droplet phase is of the order of 10^{10} , indicating that each droplet consists of ca. 10^5 PCF chains. The molar mass distribution of the droplet phase is wide, ranging from 10^7 to 10^{12} . The concentration of the concentrated droplet phase is ca. 0.4 g/cm³, and we can expect a strong intermolecular interaction among PCF chains in the concentrated phase. The solid curves in Figure 2-7 are also theoretical curves calculated by eqs. 6 – 10 with the fitting parameters listed in Table 2-II. The fitting parameters indicate that the molar mass distribution of the droplet phase becomes slightly wider and the smaller droplet phase increases upon cooling.

Table 2-II. Fitting parameters characterizing the concentrated droplet phase in solutions of sample PCF2-1 with $\phi_{\text{MeOH}} = 0.5$.

$c/10^{-7} \text{ g cm}^{-3}$	temperature/ $^{\circ}\text{C}$	$M_w/10^{10}$	M_w/M_n	$c_d/\text{g cm}^{-3}$
2.0, 4.1	40	2.0	20	0.43
6.0	40	5.0	20	0.42
6.0	15	5.0	50	0.42

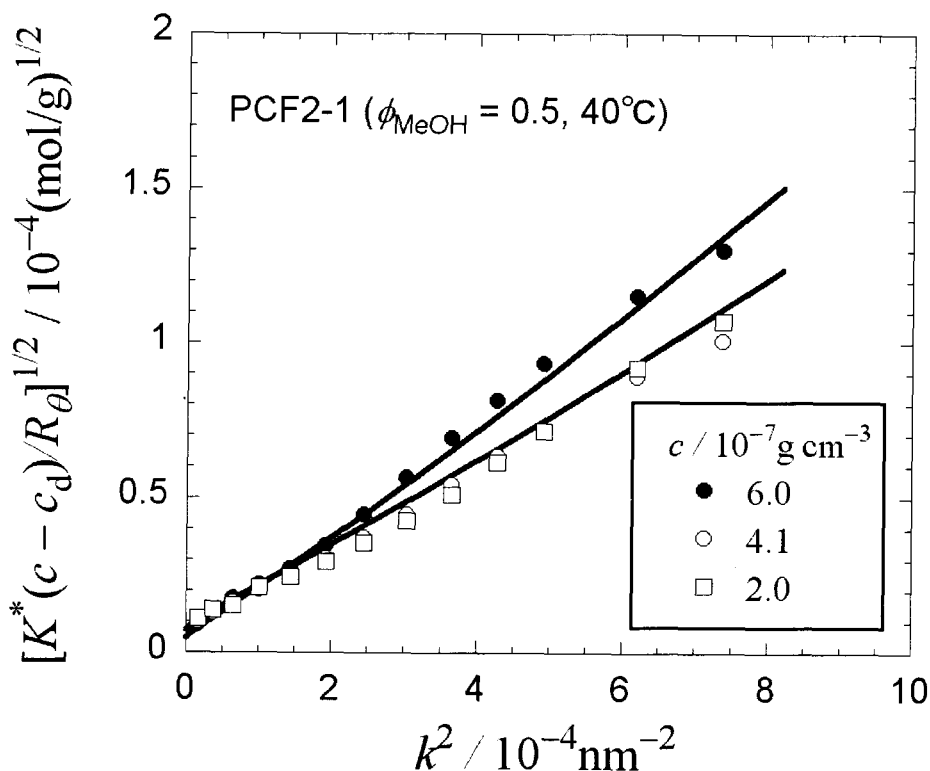


Figure 2-8. Angular dependences of $[K^*(c - c_d)/R_\theta]^{1/2}$ for concentrated droplet phases in solutions of sample PCF2-1 with $\phi_{\text{MeOH}} = 0.5$ and three different c at 40°C ; solid curves, calculated by eqs. 6 – 10 with the fitting parameters listed in Table 2-II.

It was verified that the anisotropic light scattering intensity is almost zero for the phase-separating solution of PCF with $c \sim 10^{-6} \text{ g/cm}^3$ and $\phi_{\text{MeOH}} = 0.5$. This indicates that the concentrated phase may not be the liquid-crystalline phase.

The concentration c_c is much higher than the overlap concentration of sample PCF2-1 ($\sim 10^{-3} \text{ g/cm}^3$; cf. Table 2-I), and the PCF chains are highly entangled with each other in the concentrated phase. Therefore, the helical sense conversion in PCF chains is rather difficult, which may be responsible for the slow CD induction demonstrated in Figure 2-4.

2.3.4 Intermolecular Chiral Interaction and CD Induction

According to the molecular orbital calculation and molecular modeling,^{8, 9} the polyfluorene chain favorably takes a 5/2 or 5/1 helical conformation. However, PCF did not exhibit circular dichroism in a dilute THF solution near room temperature.^{6, 7} This indicates that PCF chains take right- and left-handed helical conformations with equal probability. On the other hand, in phase-separating THF solutions of PCF by adding methanol, the right- and left-handed helical conformations are discriminated to induce CD due to polyfluorene main-chain absorption. This chiral discrimination may come from some chiral interaction among PCF chains in the separating concentrated droplet phase.

Applying McLachlan's general theory²⁵⁻²⁸ of dispersion interaction,

Osipov²⁹⁻³¹ formulated the chiral attractive interaction potential w^* between two chiral objects as follows:

$$w^* = -\frac{J^*}{p^7} \left[(\mathbf{a} \cdot \mathbf{a}') - 6 \left(\mathbf{a} \cdot \frac{\mathbf{p}}{p} \right) \left(\mathbf{a}' \cdot \frac{\mathbf{p}}{p} \right) \right] \left(\mathbf{a} \times \mathbf{a}' \cdot \frac{\mathbf{p}}{p} \right) \quad (11)$$

where \mathbf{a} and \mathbf{a}' are unit vectors parallel to the principal axes of the two objects, \mathbf{p} is the distance vector between the centers of mass of the two objects (see Figure 2-9), and J^* is the interaction strength calculated by

$$J^* \approx \frac{6\hbar\nu^2}{16\pi^2} \int_0^\infty d\omega \frac{[\varepsilon_m^2 + \varepsilon_m(\varepsilon_{||} - 3\varepsilon_\perp) + \varepsilon_{||}\varepsilon_\perp] [(2g_{||} - g_\perp)\varepsilon_m - g_\perp]}{\varepsilon_m(\varepsilon_m + \varepsilon_\perp)^3} \quad (12)$$

Here, \hbar is the Dirac constant, ν is the segment volume, ω is the angular frequency, ε_m , $\varepsilon_{||}$, and ε_\perp are the solvent permittivity and the longitudinal and transverse components of the segment permittivity, respectively, and $g_{||}$ and g_\perp are the longitudinal and transverse components of the segment gyration tensor, respectively. w^* is a short range interaction proportional to p^{-7} . Equation 12 may govern the solvent dependence of the induced CD.⁷

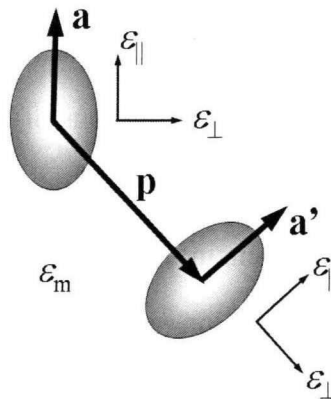


Figure 2-9. Schematic diagram of two interacting chiral objects

The right- or left-handed helical conformation of the PCF chain provides the chirality. Therefore, helical segments of the PCF chain can be regarded as chiral objects, and the chiral interaction w^* given by eq. 11 is expected among the segments. Although w^* should be zero if the segment orientation is perfectly isotropic, we may expect non-zero w^* because of the local anisotropic orientation of the segments due to the anisotropic interaction at close approach.

From symmetry, w^* between right-handed helical segments must be the same magnitude as, and opposite in sign to, that between left-handed helical segments; also, $w^* = 0$ between right- and left-handed helical segments. Thus, in the solution of PCF where the fraction of the right-handed helical segment is f_p , the average w^* should be proportional to $2f_p - 1$ of the solution.

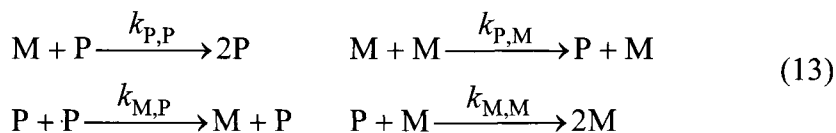
Including the entropic term, the difference ΔG_h in the free energy between right- and left-handed helical segments may be written in the form

$$\Delta G_h = \kappa(2f_p - 1) \quad (12)$$

where κ is the proportional constant, and its sign is determined by the intrinsic chirality of the PCF chain, i.e., its chiral side chain. Lifson et al.³² calculated f_p on the basis of the one-dimensional Ising model. Their theory includes three fitting parameters, ΔG_h , the free energy ΔG_r of the helix reversal, and the number of segments N_0 per chain. Now, we choose the repeating unit of PCF as the segment; $N_0 = 280$ for sample PCF2-1.

Although we have no information about ΔG_r for the PCF chain, here we choose a value of 10 kJ/mol for ΔG_r . This is the typical ΔG_r value for helical polymers like polyacetylene or polyisocyanate derivatives.^{20, 33} Figure 2-10 displays the temperature dependence of $2f_p - 1$ for three different κ on the basis of the Ising model. It can be seen that $2f_p - 1$ sharply increases with decreasing temperature below some critical value. The strong temperature dependence of the induced CD in Figure 2-3 seems to be consistent with this theoretical result.

When the helical sense conversion of the PCF segment occurs through the segment-segment interaction, there are four elementary reaction processes:



where P and M represent the right- and left-handed helical states of each segment, and $k_{\text{P,P}}$, $k_{\text{P,M}}$, $k_{\text{M,P}}$, and $k_{\text{M,M}}$ are rate constants of the elementary reactions. If those elementary reaction rates are determined only by the energies of the initial and final states, we have the relations $k_{\text{P,P}} = k_{\text{P,M}} (\equiv k_{\text{P}})$ and $k_{\text{M,P}} = k_{\text{M,M}} (\equiv k_{\text{M}})$ from the above symmetry argument on w^* . Using these relations, we finally obtain the following kinetic equation of the first-order reaction

$$2f_p - 1 = \frac{k_p - k_M}{k_p + k_M} \{1 - \exp[-(k_p + k_M)t]\} \quad (14)$$

This is consistent with the experimental result of time evolution of g_c shown in Figure 2-4.

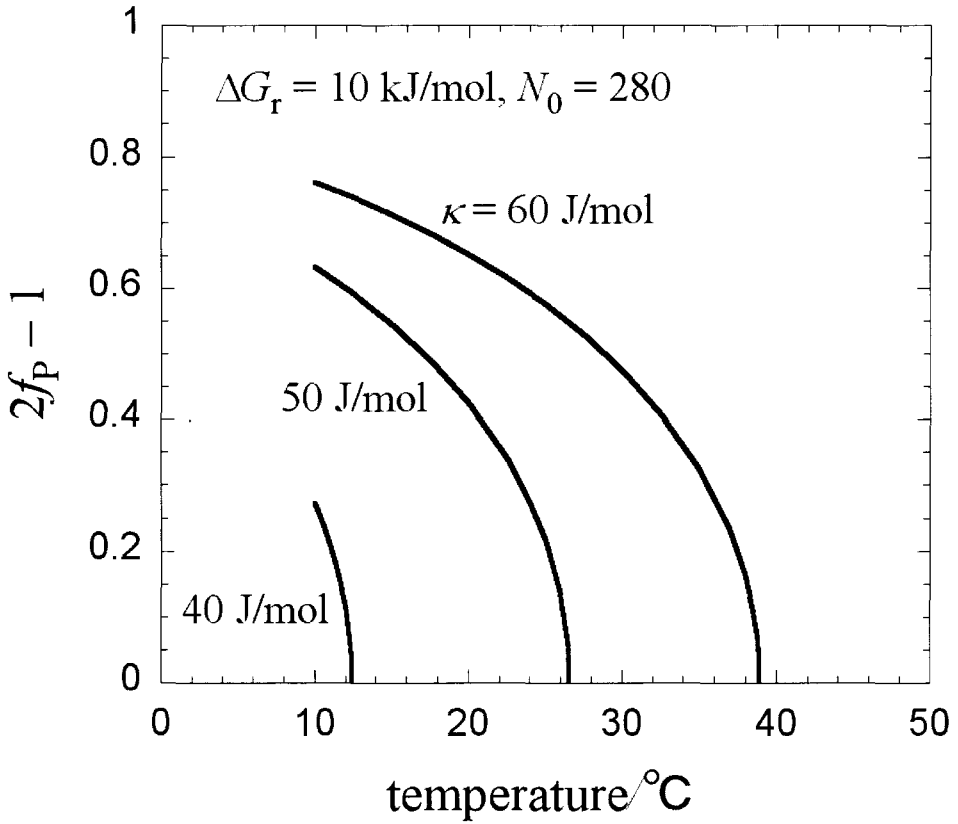


Figure 2-10. Temperature dependence of $2f_p - 1$ calculated for three different κ on the basis of the Ising model for helical polymers³¹ with $N_0 = 280$, $\Delta G_r = 10 \text{ kJ/mol}$, and eq 12.

2.4 Conclusions

We have investigated the induced CD in phase-separating solutions of an optically active polyfluorene derivative (PCF). In the phase-separating solutions, the polymer concentration of the minor concentrated phase was very high ($\sim 0.4 \text{ g/cm}^3$). The CD induction occurring in that concentrated phase was temperature sensitive and obeyed first-order reaction kinetics in the quenched solution. This was a rather slow process (the rate constant was $2.5 \times 10^{-4} \text{ s}^{-1}$).

The above experimental results can be explained by the following molecular mechanism. In the separating concentrated phase, each PCF segment feels strong chiral interactions from surrounding PCF segments. These interactions may bring about a helical sense reversal, followed by the non-racemization of PCF chains that induces CD. The helical sense conversion by the segment-segment interaction originates from the four elementary reaction processes given by eq. 13, which provide first-order reaction kinetics under a certain condition. The temperature sensitivity of the CD induction can be explained on the basis of the Ising model for helical polymers. The slow process of CD induction may be due to high entanglements among PCF chains in the concentrated phase.

2.5 References

1. Scherf, U. & Neher, D. Eds., *Polyfluorenes* (Springer, Berlin, Heiderberg, 2008).
2. Grimsdale, A. C. & Müllen, K. Polyphenylene-type Emissive Materials: Poly(para-phenylene)s, Polyfluorenes, and Ladder Polymers, *Adv. Polym. Sci.* **199**, 1 (2006).
3. Oda, M., Nothofer, H.-G., Lieser, G., Scherf, U., Meskers, S. C. J., & Neher, D. Circularly Polarized Electroluminescence from Liquid-Crystalline Chiral Polyfluorenes, *Adv. Mater.* **12**, 362-365 (2000).
4. Oda, M., Meskers, S. C. J., Nothofer, H. G., Scherf, U., & Neher, D. Chiroptical Properties of Chiral-Substituted Polyfluorenes, *Synth. Met.* **111-112**, 575-577 (2000).
5. Tang, H.-Z., Fujiki, M., & Sato, T. Thermally Driven Conformational Transition of Optically Active Poly[2,7-{9,9-bis[(S)-2-methyloctyl]}fluorene] in Solution, *Macromolecules*, **35**, 6439-6445 (2002).
6. Wu, L., Sato, T., Tang, H.-Z., & Fujiki, M. Conformation of a Polyfluorene Derivative in Solution, *Macromolecules* **37**, 6183-6188 (2004).
7. Wu, L. & Sato, T. Aggregation-Induced Circular Dichroism of Optically Active Polyfluorene Derivatives in Solution, *Kobunshi*

- Ronbunshu* **63**, 505-511 (2006).
8. Lieser, G., Oda, M., Miteva, T., Meisel, A., Nothofer, H.-G., Scherf, U., & Neher, D. Ordering, Graphoepitaxial Orientation, and Conformation of a Polyfluorene Derivative of the “Hairy-Rod” Type on an Oriented Substrate of Polyimide, *Macromolecules* **33**, 4490-4495 (2000).
 9. Hong, S. Y., Kim, D. Y., Kim, C. Y., & Hoffmann, R. Origin of the Broken Conjugation in m-Phenylene Linked Conjugated Polymers, *Macromolecules* **34**, 6474-6481 (2001).
 10. Knaapila, M. & Winokur, M. J. Structure and Morphology of Polyfluorenes in Solutions and the Solid State, *Adv. Polym. Sci.* **212**, 227-272 (2008).
 11. Lakhwani, G., Meskers, S. C. J., & Janssen, R. A. J. Circular Differential Scattering of Light in Films of Chiral Polyfluorene, *J. Phys. Chem. B* **111**, 5124-5131 (2007).
 12. Langeveld-Voss, B. M. W., Waterval, R. J. M., Janssen, R. A. J., & Meijer, E. W. Principles of “Majority Rules” and “Sergeants and Soldiers” Applied to the Aggregation of Optically Active Polythiophenes: Evidence for a Multichain Phenomenon, *Macromolecules* **32**, 227-230 (1999).
 13. Nakashima, H., Fujiki, M., Koe, J. R., & Motonaga, M. Solvent and Temperature Effects on the Chiral Aggregation of

- Poly(alkylarylsilane)s Bearing Remote Chiral Groups, *J. Am. Chem. Soc.* **123**, 1963-1969 (2001).
14. Goto, H. & Yashima, Y. Electron-Induced Switching of the Supramolecular Chirality of Optically Active Polythiophene Aggregates, *J. Am. Chem. Soc.* **124**, 7943-7949 (2002).
 15. Peng, W., Motonaga, M., & Koe, J. R. Chirality Control in Optically Active Polysilane Aggregates, *J. Am. Chem. Soc.* **126**, 13822-13826 (2004).
 16. Yamakawa, H. *Modern Theory of Polymer Solutions*. S. A. Rice, Ed. (Harper & Row, New York, 1971).
 17. Strazielle, C. in *Light Scattering from Polymer Solutions* Huglin, M. B., Ed. (Academic Press, London & New York, 1972).
 18. Flory, P. J. *Principles of Polymer Chemistry* (Cornell Univ. Press, Ithaca, New York, 1953).
 19. Dias, F. B., Morgado, J., Maçanita, A. L., da Costa, F. P., Burrows, H. D., & Monkman, A. P. Kinetics and Thermodynamics of Poly(9,9-dioctylfluorene) α -Phase Formation in Dilute Solution, *Macromolecules* **39**, 5854-5864 (2006).
 20. Sato, T., Terao, K., Teramoto, A., & Fujiki, M. Molecular properties of helical polysilylenes in solution, *Polymer* **44**, 5477-5495 (2003).
 21. Wesslau, H. Die Molekulargewichtsverteilung einiger Niederdruckpolyäthylene, *Makromol. Chem.* **20**, 111-120 (1956).

22. Brandrup, J. & Immergut, E. H. Eds., *Polymer Handbook* (John Wiley & Sons, New York, ed. 3rd, 1989).
23. Prod, G. in *Small Angle X-ray Scattering* O. Glatter, and O. Kratky, Eds. (Academic Press, London, 1982).
24. Debye, P. Light Scattering in Soap Solutions, *Ann. N.Y. Acad. Sci.* **51**, 575-592 (1949).
25. McLachlan, A. D. Retarded Dispersion Forces Between Molecules, *Proc. Roy. Soc. London* **A271**, 387-401 (1963).
26. McLachlan, A. D. Retarded Dispersion Forces in Dielectrics at Finite Temperatures, *Proc. Roy. Soc. London* **A274**, 80-90 (1963).
27. Imura, H. & Okano, K. van der Waals-Lifshitz Forces between Anisotropic Ellipsoidal Particles, *J. Chem. Phys.* **58**, 2763-2776 (1973).
28. Israelachvili, J. N. *Intermolecular and Surface Forces* (Academic Press, London, ed. 2nd, 1992).
29. Osipov, M. A. Theory for Cholesteric Ordering in Lyotropic Liquid Crystals, *Il. Nuovo Cimento D* **10**, 1249-1262 (1988).
30. Osipov, M. A. Molecular Theory of Solvent Effect on Cholesteric Ordering in Lyotropic Polypeptide Liquid Crystals, *Chem. Phys.* **96**, 259-270 (1985).
31. Osipov, M. A. in *Liquid Crystalline and Mesomorphic Polymers* V. P.

Shibaev, and L. Lam, Eds. (Springer, Berlin & Heidelberg, 1994),
Chapt. 1.

32. Lifson, S., Andreola, C., Peterson, N. C., & Green, M. M. Macromolecular Stereochemistry: Helical Sense Preference in Optically Active Polyisocyanates. Amplification of a Conformational Equilibrium Deuterium Isotope Effect, *J. Am. Chem. Soc.* **111**, 8850-8858 (1989).
33. Morino, K., Maeda, K., Okamoto, Y., Yashima, E., & Sato, T. Temperature Dependence of Helical Structures of Poly(phenylacetylene) Derivatives Bearing an Optically Active Substituent, *Chem. Eur. J.* **8**, 5112-5120 (2002).

Chapter 3.

Double Screw-Sense Inversions of Helical Chiral-Achiral Random Copolymers of Fluorene Derivatives in Phase Separating Solutions

3.1 Introduction

Recently, π - and σ -conjugated polymers, which possess interesting electrical and optical properties, have attracted much interest as candidates for organic light-emitting diodes¹⁻³ and chemical sensors.⁴ Chiroptical properties, such as circular dichroism (CD), optical rotation, and circular polarized luminescence, enrich the applications of these organic semiconductors as optical devices or sensors.⁵⁻⁹ Optically active side chains may introduce chiroptical properties into conjugated polymers, but some polymers exhibit these properties only in films or phase separating solutions,¹⁰⁻¹³ which indicates that intermolecular chiral interactions are necessary to induce the chiroptical properties in such conjugated polymers.

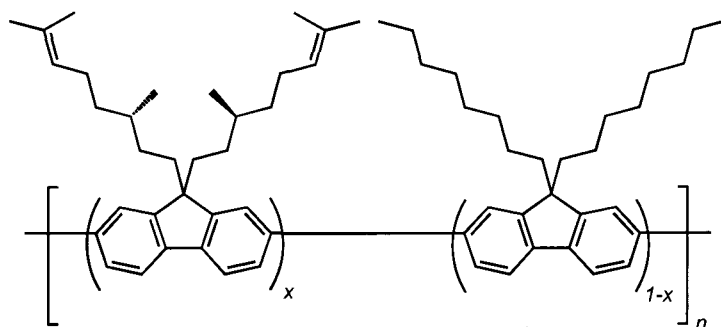
Polyfluorene derivatives are π -conjugated polymers. From electron and X-ray diffraction^{14, 15} as well as molecular modeling,^{14, 16} these polymers are known to take a helical conformation, but chirality introduced to the side chain of the polymers was not found to induce circular dichroism (CD) on their backbone chain in dilute solution. This finding

probably results from weak intramolecular chiral interactions that cannot discriminate against the handedness of the backbone helical conformation.

In the previous Chapter,¹⁷ the CD induction of an optically active homopolymer of fluorene derivative, poly(2,7-[9,9-bis((*S*-citronellyl)]fluorene) (PCF), in dilute THF solutions was found by the addition of a non-solvent methanol. Although the methanol-added solutions were almost transparent because of low polymer concentrations ($\sim 10^{-6}$ g/cm³), static light scattering measurements indicated a liquid-liquid phase separation to form concentrated droplet phases, and it was concluded that this induction arises from the intermolecular chiral interaction of polyfluorene chains in the concentrated droplet phases separated from the dilute solution.

Helical chiral-achiral random copolymers often exhibit interesting chiroptical properties, e.g., sergeants-and-soldiers behavior,¹⁸⁻²⁰ composition-driven helical screw-sense inversion,^{21, 22} and so on. Therefore, the CD induction study in phase separating solution was recently extended to a helical chiral-achiral random copolymer of fluorene derivatives, poly(2,7-[9,9-bis((*S*-citronellyl)]fluorene-*random*-9,9-di-*n*-octyl fluorene), as shown in Scheme 3-1, and double screw-sense inversions were found by changing the chiral monomer content x . To the best of our knowledge, this is the first observation of composition-driven double sense inversions in

helical chiral-achiral random copolymers. In this Chapter, this finding is reported along with the theoretical argument of its origin.



Scheme 3-1. Chemical structure of the chiral-achiral random copolymer studied.

3.2 Experimental Section

3.2.1 Samples

Mixtures of the chiral and achiral dibromofluorene monomers of different compositions were copolymerized in a hot mixture of toluene and *N,N*-dimethylformamide (DMF) using a zero-valent nickel reagent by the Yamamoto coupling reaction.⁷ Each copolymer sample was divided into three fractions by fractional precipitation using THF as the solvent and methanol as the precipitant, and the middle main fraction was chosen for the following experiments.

The chiral monomer content x of five middle copolymer fractions was estimated from the ratio of the integrated intensities of the proton signals of the chiral side chains and aromatic rings. The results, listed in Table 3-I,

are very close to the compositions fed at the copolymerization (the numbers in the parentheses in the second column of Table 3-I). The weight average molecular weights, M_w , and the ratios of M_w to the number average, M_n , of the five fractions were determined by size-exclusion chromatography with a multi-angle light scattering detector (SEC-MALS).²³ Table 3-I lists the results and weight average degree of polymerization $N_{0,w}$ calculated from the M_w determined. The values of M_w/M_n indicate the relatively narrow molecular weight distributions of the fractions used in this study. One fraction of the chiral homopolymer PCF prepared in the previous Chapter was added to the copolymer fractions for the following CD induction study, and its M_w was determined by static light scattering (SLS).¹⁷ The values of $N_{0,w}$ of all the fractions were within the range of ca. 100–300.

Table 3-I. Characteristics of polymer fractions used in this study and of concentrated droplet phases in methanol-added THF solutions of fractions PC5O5 and PCF.

Fraction	x	$M_w/10^4$	$N_{0,w}$	M_w/M_n^c	R_w/nm^d	R_w/R_n^d	$c_c/gcm^{-3}d$
PC8O2	0.80 ^a (0.8 ^b)	11.5 ^c	267	1.5			
PC6O4	0.60 ^a (0.6 ^b)	4.1 ^c	98	1.3			
PC5O5	0.50 ^a (0.5 ^b)	7.0 ^c	169	1.4	110 ^e (83 ^f)	1.4 ^e (1.3 ^f)	0.60 ^e (0.59 ^f)
PC2O8	0.19 ^a (0.2 ^b)	10.5 ^c	264	1.5			
PCF	1.0 (1.0 ^b)	13.4 ^d	305	-	150 ^e (170 ^f)	1.8 ^e (1.8 ^f)	0.50 ^e (0.50 ^f)

^a Determined by ¹H NMR. ^b Chiral monomer composition fed at the polymerization.

^c Determined by SEC-MALS. ^d Determined by SLS. ^e at 15 °C. ^f at 40 °C.

3.2.2 Measurements

Each fraction was first dissolved in THF ($8 \times 10^{-7} \text{ g/cm}^3$), and then, methanol was added to the THF solution at room temperature. The methanol volume fraction ϕ_{MeOH} in the mixed solvent and the final polymer concentration c in the THF-methanol solution were adjusted to 0.5 and $4 \times 10^{-7} \text{ g/cm}^3$, respectively. CD and SLS measurements were conducted using the THF-methanol solutions prepared using a JASCO J-720WO spectropolarimeter and a Fica 50 light scattering photogoniometer with 546 nm incident light, respectively, at 40 and 15 °C.

3.3 Results

3.3.1 Static Light Scattering

Figure 3-1 shows the light scattering profiles of THF-methanol solutions of fractions PC5O5 ($x = 0.50$) and PCF ($x = 1$) at 40 °C and 15 °C (300 min after quenching from 40 °C). Here, K is the optical constant, c is the polymer mass concentration, R_θ is the excess Rayleigh ratio at the scattering angle θ , and k^2 is the square of the scattering vector. All of the profiles exhibit very strong angular dependences, demonstrating the existence of large particles in the solutions. The phase diagram obtained previously for the methanol-added THF solution of PCF indicates that the solutions may be in the biphasic region, and the large particles are the concentrated droplet phases separated from the dilute solutions.

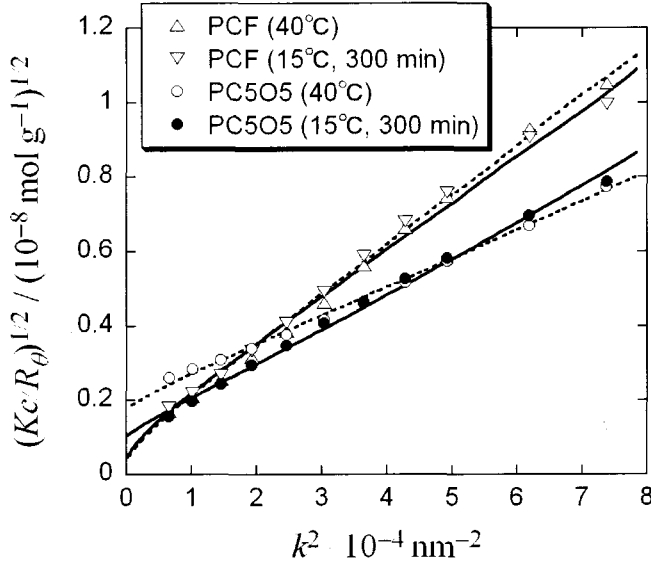


Figure 3-1. Berry plots for methanol-added THF solutions of fractions PC505 ($x = 0.50$) and PCF ($x = 1$) at 40 °C and 15 °C (300 min after quenching from 40 °C); $\phi_{\text{MeOH}} = 0.5$ and $c = 4 \times 10^{-6} \text{ g/cm}^3$. Solid and dotted curves, theoretical values for polydisperse spheres fitted to the data at 15 and 40 °C, respectively (see the main text).

For dilute solutions of polydisperse spheres, $(Kc/R_\theta)^{1/2}$ can be calculated by¹⁷

$$\frac{R_\theta}{Kc} = \frac{12\pi N_A c_c}{k^3} \int_0^\infty \frac{[\sin(kR) - kR \cos(kR)]^2}{(kR)^3} w(R) dR \quad (1)$$

where R is the radius of the sphere, $w(R)$ is the weight fraction of a sphere of radius R , c_c is the polymer mass concentration in the spherical concentrated phase, and N_A is the Avogadro constant. Assuming that the size distribution $w(R)$ obeys the log-normal distribution,¹⁷ Eq. 1 was fitted

to the experimental results to obtain the weight-average radius R_w , the ratio of R_w to the number-average R_n of the droplet phase and c_c . The solid and dotted curves in Figure 3-1 show the fitting results, and the parameters obtained are listed in columns 5 – 8 in Table 3-I. Droplet sizes are on order of 100 nm. The concentrations of the droplet phases are as high as 0.6 g/cm³ for both fractions and almost independent of temperature. The results of c_c for fractions PC5O5 and PCF indicate the similar affinities of the chiral and achiral monomer units to the mixed solvent.

3.3.2 Circular Dichroism Induction

None of the copolymer fractions exhibited CD in dilute THF solution, as in the case of the chiral homopolymer PCF,¹⁷ which indicates that the *intramolecular* chiral interaction between the main and side chains of the copolymers is too weak to energetically discriminate the right- and left-handed helical conformations in the fluorene main chain.

Figure 3-2 shows UV-visible absorption and CD spectra of the phase separating solution of PC5O5 quenched from 40 to 15 °C. In Panel A, the main peak of the UV-visible absorption, arising from the $\pi-\pi^*$ transition in the fluorene main chain, is essentially unchanged over time since quenching, but the peak height decreases, the peak wavelength slightly increases, and a new side-peak appears at 426 nm. On the other hand, a bisign CD signal is induced in the fluorene main-chain absorption region

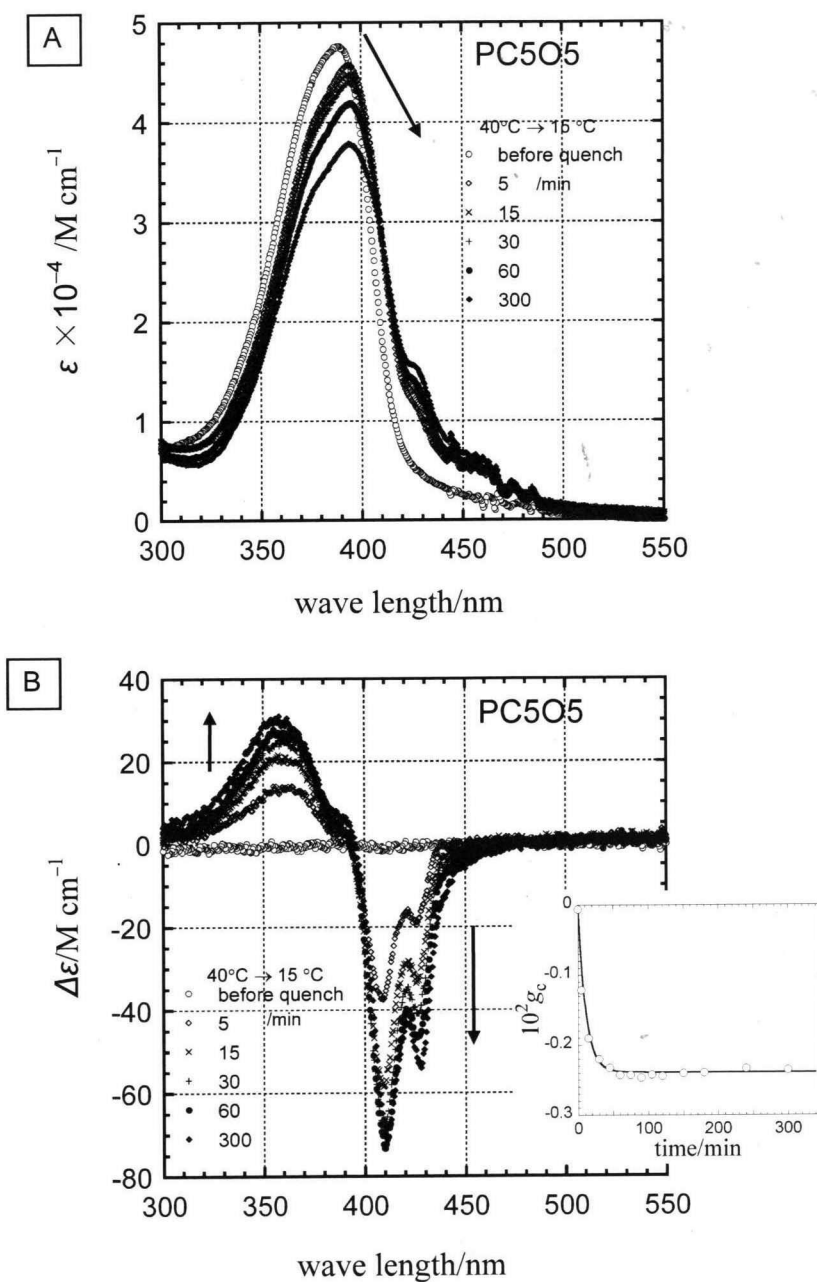


Figure 3-2. Spectra of the molar circular dichroism $\Delta\varepsilon$ and the average molar extinction coefficient ε for methanol-added THF solution of fraction PC5O5; inset in Panel B: time dependence of the Kuhn

by quenching in Panel B, just as in the case of fraction PCF reported previously. The induced CD disappeared upon heating to 40 °C and reappeared by quenched again to 15 °C, which is similar to PCF and demonstrates the thermal reversibility of the CD induction. The phase-separating solutions were verified to have no optical anisotropy,¹⁷ which means that the induced CD does not arise from a liquid crystal phase. The polyfluorene chain is known to take 5/2 or 5/1 helical conformations favorably^{14, 16} so that the CD induction indicates uneven population of the right- and left-handed helical conformations of the copolymer main-chain. The Kuhn dissymmetry factor $g_c \equiv \Delta\epsilon/\epsilon$ at 410 nm (the CD peak position) reaches the asymptotic value at approximately 60 min (cf. Insert of Figure 3-1), which is slightly faster than g_c of the PCF solution.¹⁷

The new side peak at 426 nm in Panel A corresponds to the so-called " β -phase" observed for poly(9,9-di-*n*-octylfluorene) films,^{24, 25} which is assigned to an almost planar conformation of the fluorene main chain with the torsional angle $\approx 160^\circ$ stabilized by the *n*-octyl side chains.²⁶ A more pronounced side-peak was observed in the methanol-added THF solution of fraction PC2O8, indicating that some of achiral monomer units take similar planer conformations in the concentrated droplet phase. Interestingly, a side-peak also grows in the CD spectrum (Panel B) at the same wavelength, which may arise from the achiral monomer unit in the copolymer chain taking the " β -phase" conformation.

In the methanol-added THF solution with the same ϕ_{MeOH} and c , a similar CD induction was observed for PC6O4 quenched from 40 to 15 °C, but a CD signal appeared for PC2O8 even at 40 °C and did not change with time after quenching to 15 °C. The CD induction experiments were examined twice for fraction PC2O8, and nearly the same CD spectra were obtained, confirming the reproducibility of the CD induction for this fraction.

Figure 3-3 shows the asymptotic CD absorption spectra for all chiral-achiral random copolymers and the chiral homopolymer PCF in methanol-added THF solutions ($\phi_{\text{MeOH}} = 0.5$, $c = 4 \times 10^{-7} \text{ g/cm}^3$). The bisign CD main signals induced in PCF and PC2O8 solutions are positive in the longer wavelength region but opposite in PC6O4 and PC5O5 solutions, and PC8O2 exhibits almost no CD. The sign of the side peak of PC2O8 (at 429 nm) is also opposite to that of PC5O5 (at 426 nm). The insert in Figure 3-3 shows the x dependence of the Kuhn dissymmetry factor at the CD peak in the region of 400 – 420 nm. These results demonstrate that the helical screw sense of the chiral-achiral random copolymer is inverted twice with changing x . To the best of our knowledge, this is the first observation of the double sense inversions in helical chiral-achiral random copolymers.

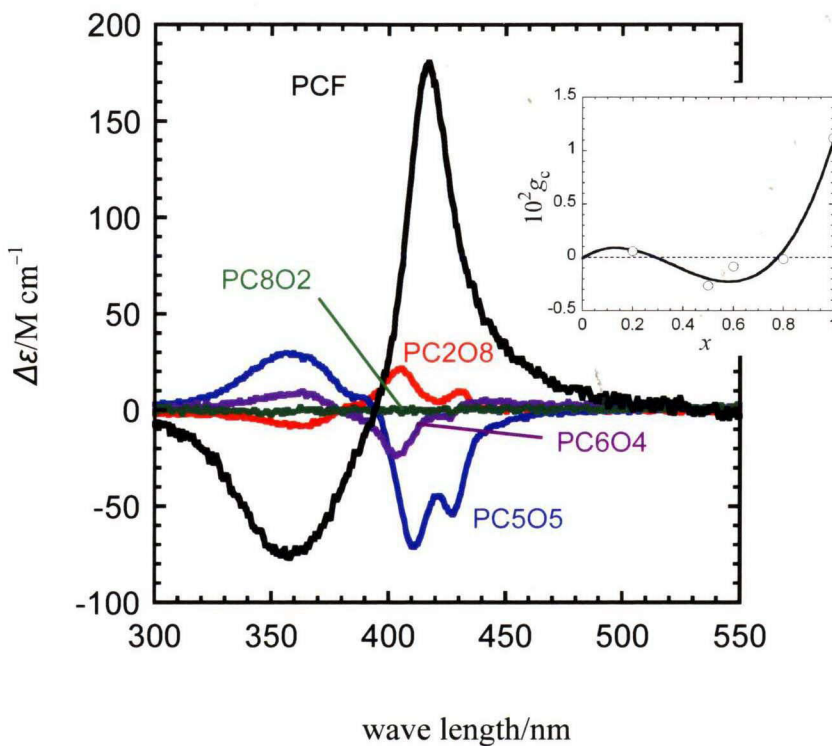


Figure 3-3. Asymptotic CD absorption spectra for all chiral-achiral random copolymers and the chiral homopolymer PCF in methanol-added THF solutions; inset: the x dependence of the Kuhn dissymmetry factor at the CD peak in the region of 400 – 420 nm.

3.4 Discussion

Consider the origin of the double sense inversions in helical chiral-achiral random copolymers. For simplicity, assume that the main-chain bond (i.e., the internal rotation angle) of the helical polymer chain takes P- or M-states (a two-state model). The P-helix (M-helix) means the sequence of main-chain bonds taking the P-state (M-state). In a concentrated solution

a bond taking the P-state (M-state) feels the chiral molecular field $\bar{w}^*(P)$ ($\bar{w}^*(M)$) generated by neighboring polymer molecules.²⁷ If the solution contains P- and M-state bonds of fractions f_P and f_M , respectively, the molecular fields, $\bar{w}^*(P)$ and $\bar{w}^*(M)$, may be given by

$$\bar{w}^*(P) = w_{PP}^* f_P + w_{PM}^* f_M, \quad \bar{w}^*(M) = w_{PM}^* f_P + w_{MM}^* f_M \quad (2)$$

where w_{PP}^* , w_{MM}^* , and w_{PM}^* are the chiral interactions between two pairs of adjacent monomer units connected by the bonds both taking the P-state, both taking the M-state, and taking the P- and M-states, respectively. Because the molecular field may include both enthalpic and entropic contributions, $\bar{w}^*(P) - \bar{w}^*(M)$ can be regarded as the free energy difference $2\Delta G_h$ of a bond when taking the P-state and M-state in the concentrated solution. From Eq. 2, ΔG_h is a linear function of the enantiomer excess $2f_P - 1$, i.e., $\Delta G_h = \kappa(2f_P - 1) + \lambda$ where κ and λ are parameters related to the chiral interactions. In the previous Chapter, it was assumed that $\lambda = 0$, but w_{PP}^* and w_{MM}^* are not necessarily identical unless the interacting monomer units are both achiral.

In the case of a chiral-achiral random copolymer solution, ΔG_h may depend on the kinds of adjacent monomer units connected by the bond under consideration:²⁸

$$\begin{aligned} \Delta G_{h,CC} &= \kappa_{CC} (2f_P - 1) + \lambda_{CC}, \quad \Delta G_{h,CA} = \kappa_{CA} (2f_P - 1) + \lambda_{CA}, \\ \Delta G_{h,AA} &= \kappa_{AA} (2f_P - 1) \end{aligned} \quad (3)$$

where the subscripts C and A denote the chiral and achiral monomer units, respectively. Because the achiral homopolymer should be racemic at $2f_P - 1 = 0$, λ_{AA} must be zero. Helical polymers must have long sequences of the one-sense helical state along the main chain, or the helix reversal must be a rare event. Thus, the free energy ΔG_r of the helix reversal, where the adjacent bonds take the opposite helical state, must be quite high.²⁹ In what follows, the dependence of ΔG_r on the kinds of adjacent monomer units connected by the bond under consideration is not considered, which should have a minor effect on the helical screw sense inversion.

The enantiomer excess $2f_P - 1$ of the chiral-achiral random copolymer chain can be calculated by the matrix method for the Ising model.^{28, 30, 31} The matrix includes the statistical weights of the P- and M-states and the helix reversal, which are respectively written as

$$\begin{cases} u_{P,i(k)i(k+1)} = \exp(\Delta G_{h,i(k)i(k+1)}/RT) \\ u_{M,i(k)i(k+1)} = \exp(-\Delta G_{h,i(k)i(k+1)}/RT) \\ \nu = \exp(-\Delta G_r/RT) \end{cases} \quad (4)$$

where the subscripts $i(k)$ ($1 \leq k \leq N$), taking C (the chiral monomer unit) or A (the achiral monomer unit), specify the copolymer sequence and RT is the gas constant multiplied by the absolute temperature. (This R should be distinguished from the radius R in Eq. 1.) Generating 100 sequences of chiral-achiral random copolymers with a given N and mole fraction x of the

chiral unit on a computer, $2f_p - 1$ can be calculated numerically for the given values of $\Delta G_{h,CC}$, $\Delta G_{h,CA}$, $\Delta G_{h,AA}$, and ΔG_r in the routine procedure.

The calculated $2f_p - 1$ must fulfill Eqs. 3 for $\Delta G_{h,CC}$, $\Delta G_{h,CA}$, and $\Delta G_{h,AA}$. This self-consistent calculation can be performed as follows. From Eqs. 3, the relations among $\Delta G_{h,CC}$, $\Delta G_{h,CA}$, and $\Delta G_{h,AA}$ are obtained:

$$\Delta G_{h,CA} = \frac{\kappa_{CA}}{\kappa_{CC}}(\Delta G_{h,CC} - \lambda_{CC}) + \lambda_{CA}, \quad \Delta G_{h,AA} = \frac{\kappa_{AA}}{\kappa_{CC}}(\Delta G_{h,CC} - \lambda_{CC}) \quad (5)$$

A trial value of $\Delta G_{h,CC}$ is chosen first, and $\Delta G_{h,CA}$ and $\Delta G_{h,AA}$ are calculated from Eqs. 5 using a given set of the parameters κ_{CA}/κ_{CC} , κ_{AA}/κ_{CC} , λ_{CC} , and λ_{CA} . Then, $2f_p - 1$ is calculated by the matrix method using those values of ΔG_h and a given value of ΔG_r , and the resulting $2f_p - 1$ is substituted into the first equation of Eqs. 3 to check the equality. The self-consistent value of $\Delta G_{h,CC}$ that fulfills the equation is sought.

The previous result in Chapter 2 indicated that $2f_p - 1$ for PCF in the phase-separating solution is close to zero at 40 °C but takes a positive finite value at 15 °C.¹⁷ To reproduce these results, $\kappa_{CC} = 40$ J/mol and $\lambda_{CC} = 2$ J/mol were selected (using these parameters, $2f_p - 1$ for PCF becomes 0.09 at 40 °C and 0.38 at 15 °C). Furthermore, $N = 220$ (the average value of our five polymer fractions) and $\Delta G_r = 10$ kJ/mol (a typical value for helical polymers such as polyacetylene or polyisocyanate derivatives^{32, 33}). The remaining parameters in Eqs. 2, κ_{CA} , κ_{AA} , and λ_{CA} , were taken as adjustable parameters. (The κ and λ parameters may depend on the polymer

concentration c_c in the concentrated phase, but here it is assumed that these parameters are independent of x because c_c may be insensitive to x due to similar affinities of the chiral and achiral monomer units to the mixed solvent, mentioned above.)

Figure 3-4 shows the results of $2f_P - 1$ at 15 °C as a function of $\Delta G_{h,CC}$ and x for $\kappa_{CA}/\kappa_{CC} = -2.5$, $\kappa_{AA}/\kappa_{CC} = 3.5$, $\lambda_{CC} = 2$ J/mol, and $\lambda_{CA} = -4$ J/mol.

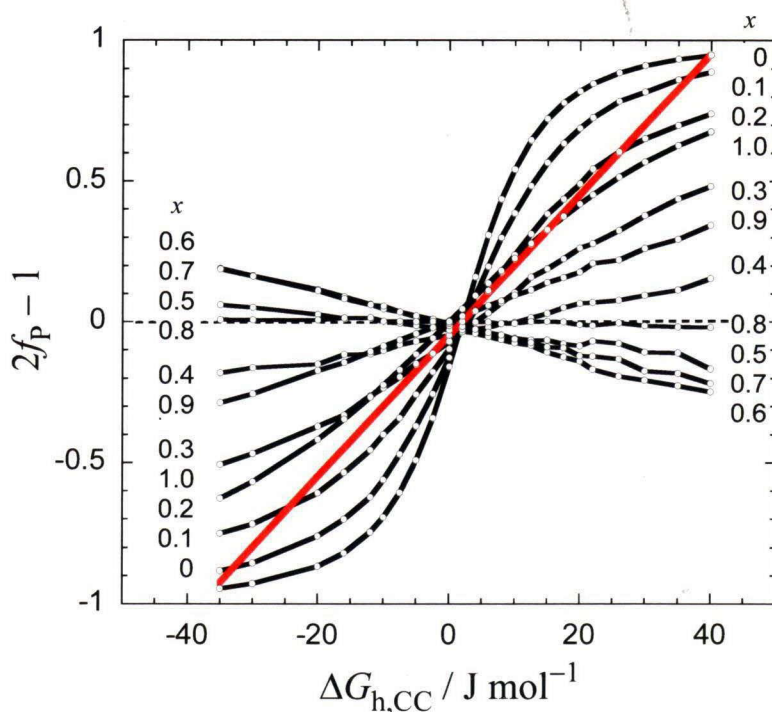


Figure 3-4. Enantiomer excess as a function of $\Delta G_{h,CC}$ and x , calculated by the matrix method for the Ising model of the random copolymer with $\kappa_{CA}/\kappa_{CC} = -2.5$, $\kappa_{AA}/\kappa_{CC} = 3.5$, $\lambda_{CC} = 2$ J/mol, $\lambda_{CA} = -4$ J/mol, $\Delta G_r = 10$ kJ/mol, $N = 220$, and $T = 288$ K (15 °C).

Slight fluctuations in the calculated $2f_p - 1$ values arise from statistical errors in the chiral monomer content generated. The straight line in Figure 3-4 represents the linear relation of $2f_p - 1 = (\Delta G_h - \lambda_{CC})/\kappa_{CC}$ with $\kappa_{CC} = 40$ J/mol. The intersecting point of this line and the curve for each x fulfills Eqs. 3. At large x , the curve intersects with the line once, but, in the small x region, there are three intersecting points.

Figure 3-5 shows the self-consistent solution of $2f_p - 1$ at 15 °C, obtained from Figure 3-4, as a function of x . At large x (> 0.227), the calculation gives the unique self-consistent solution of $2f_p - 1$. When x decreases from unity, $2f_p - 1$ changes from positive to negative (the

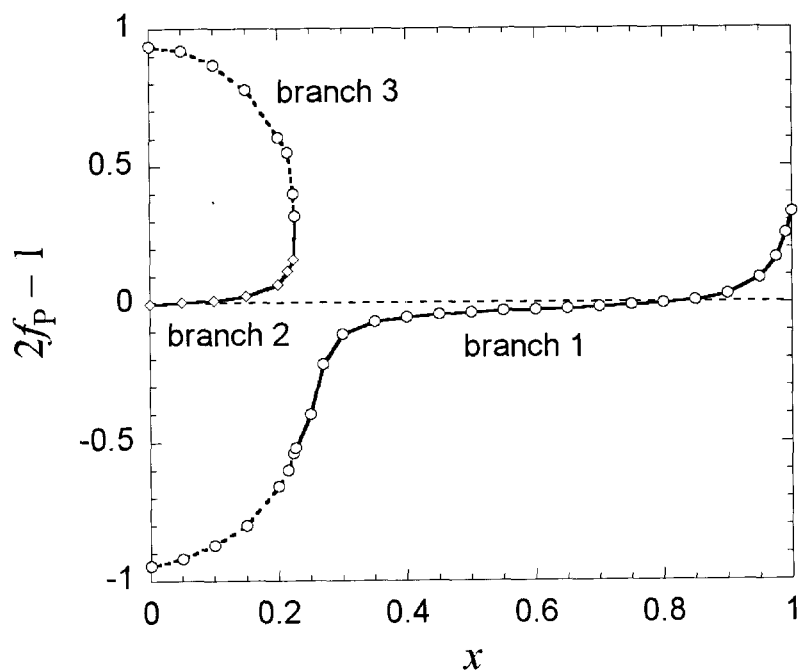


Figure 3-5. Self-consistent solutions of the enantiomer excess $2f_p - 1$ as a function of x for the parameters listed in the text.

solution of branch 1), corresponding to the first helical screw sense inversion. However, one negative and two positive solutions appear at $x < 0.227$. Among these solutions, the positive one reaching the origin (labeled as the branch 2) should be the real solution because the achiral homopolymer must be racemic. Therefore, a transition from branch 1 to 2 is expected with decreasing x , which corresponds to the second helical screw sense inversion. This *discontinuous* transition is an interesting phenomenon. The CD induction at x between 0.2 and 0.5 will be studied experimentally in more detail in the near future.

3.5 Conclusions

Methanol-added THF solutions of chiral-achiral random copolymers of fluorene derivatives with different chiral monomer content x were studied. The addition of methanol to dilute THF solutions of the copolymers and the chiral homopolymer induced a liquid-liquid phase separation that produced concentrated phase droplets with a polymer concentration as high as 0.6 g/cm^3 and a size of the order of 100 nm. In the concentrated phase, the copolymers and homopolymer exhibited mostly thermo-reversible circular dichroism (CD) induction after quenching in the main-chain fluorene absorption region, demonstrating the uneven population of the right- and left-handed helical conformation in the polymer chains. From the sign of the induced CD, two helical screw-sense

inversions were found by changing x . The Ising model for chirally interacting chiral-achiral random copolymers can explain the double screw-sense inversions.

3.6 References

1. Burroughes, J.H., Bradley, D.D.C., Brown, A.R., Marks, R.N., Mackay, K., Friend, R.H., Burns, P.L. & Holmes, A.B. Light-Emitting Diodes Based on Conjugated Polymers *Nature* **347**, 539-541 (1990).
2. Scherf, U. & Neher, D., eds. Polyfluorenes. *Adv. Polym. Sci.* 2008, Springer: Berlin, Heiderberg.
3. Grimsdale, A.C. & Müllen, K. Polyphenylene-type Emissive Materials: Poly(para-phenylene)s, Polyfluorenes, and Ladder Polymers *Adv. Polym. Sci.* **199**, 1-82 (2006).
4. McQuade, D.T., Pullen, A.E. & Swager, T.M. Conjugated Polymer-Based Chemical Sensors *Chem. Rev.* **100**, 2537-2574 (2000).
5. Oda, M., Nothofer, H.-G., Lieser, G., Scherf, U., Meskers, S.C.J. & Neher, D. Circularly Polarized Electroluminescence from Liquid-Crystalline Chiral Polyfluorenes *Adv. Mater.* **12**, 362-365 (2000).
6. Oda, M., Meskers, S.C.J., Nothofer, H.G., Scherf, U. & Neher, D. Chiroptical properties of chiral-substituted polyfluorenes *Synth. Met.* **111-112**, 575-577 (2000).

7. Tang, H.-Z., Fujiki, M. & Sato, T. Thermally Driven Conformational Transition of Optically Active Poly[2,7-{9,9-bis[(S)-2-methyloctyl]}fluorene] in Solution *Macromolecules* **35**, 6439-6445 (2002).
8. Wu, L., Sato, T., Tang, H.-Z. & Fujiki, M. Conformation of a Polyfluorene Derivative in Solution *Macromolecules* **37**, 6183-6188 (2004).
9. Wu, L. & Sato, T. Aggregation-Induced Circular Dichroism of Optically Active Polyfluorene Derivatives in Solution *Kobunshi Ronbunshu* **63**, 505-511 (2006).
10. Langeveld-Voss, B.M.W., Waterval, R.J.M., Janssen, R.A.J. & Meijer, E.W. Principles of "Majority Rules" and "Sergeants and Soldiers" Applied to the Aggregation of Optically Active Polythiophenes: Evidence for a Multichain Phenomenon *Macromolecules* **32**, 227-230 (1999).
11. Nakashima, H., Fujiki, M., Koe, J.R. & Motonaga, M. Solvent and Temperature Effects on the Chiral Aggregation of Poly(alkylarylsilane)s Bearing Remote Chiral Groups *J. Am. Chem. Soc.* **123**, 1963-1969 (2001).
12. Goto, H. & Yashima, Y. Electron-Induced Switching of the Supramolecular Chirality of Optically Active Polythiophene Aggregates *J. Am. Chem. Soc.* **124**, 7943-7949 (2002).

13. Peng, W., Motonaga, M. & Koe, J.R. Chirality Control in Optically Active Polysilane Aggregates *J. Am. Chem. Soc.* **126**, 13822-13826 (2004).
14. Lieser, G., Oda, M., Miteva, T., Meisel, A., Nothofer, H.-G., Scherf, U. & Neher, D. Ordering, Graphoepitaxial Orientation, and Conformation of a Polyfluorene Derivative of the "Hairly-Rod" Type on an Oriented Substrate of Polyimide *Macromolecules* **33**, 4490-4495 (2000).
15. Knaapila, M. & Winokur, M.J. Structure and Morphology of Polyfluorenes in Solutions and the Solid State *Adv. Polym. Sci.* **212**, 227-272 (2008).
16. Hong, S.Y., Kim, D.Y., Kim, C.Y. & Hoffmann, R. Origin of the Broken Conjugation in m-Phenylene Linked Conjugated Polymers *Macromolecules* **34**, 6474-6481 (2001).
17. Sanada, Y. & Sato, T. Induced Circular Dichroism of an Optically Active Polyfluorene Derivative in Phase-Separating Solutions *Polym. J.* **42**, 195-200 (2010).
18. Green, M.M., Reidy, M.P., Johnson, R.D., Darling, G., O'Leary, D.J. & Wilson, G. Macromolecular Stereochemistry: The Out-of-Proportion Influence of Optically Active Comonomers on the Conformational Characteristics of Polyisocyanates: The Sergeants & Soldiers Experiment *J. Am. Chem. Soc.* **111**, 6452-6454 (1989).

19. Green, M.M., Peterson, N.C., Sato, T., Teramoto, A., Cook, R. & Lifson, S. A Helical Polymer with Cooperative Response to Chiral Information *Science* **268**, 1860-1866 (1995).
20. Green, M.M., Park, J.-W., Sato, T., Teramoto, A., Lifson, S., Selinger, R.L.B. & Selinger, J.V. The Macromolecular Route to Chiral Amplification *Angew. Chem. Int. Ed.* **38**, 3138-3154 (1999).
21. Maeda, K. & Okamoto, Y. Synthesis and Conformational Characteristics of Poly(phenyl isocyanate)s Bearing an Optically Active Ester Group *Macromolecules* **32**, 974-980 (1999).
22. Koe, J.R., Fujiki, M., Motonaga, M. & Nakashima, H. Cooperative Helical Order in Optically Active Poly(diarylsilylenes) *Macromolecules* **34**, 1082-1089 (2001).
23. Matsuda, Y., Biyajima, Y. & Sato, T. Thermal Denaturation, Renaturation, and Aggregation of a Double-Helical Polysaccharide Xanthan in Aqueous Solution *Polym. J.* **41**, 526-532 (2009).
24. Grell, M., Bradley, D.D.C., Ungar, G., Hill, J. & Whitehead, K.S. Interplay of Physical Structure and Photophysics for a Liquid Crystalline Polyfluorene *Macromolecules* **32**, 5810-5817 (1999).
25. Knaapila, M. & Winokur, M.J. Structure and Morphology of Polyfluorenes in Solutions and the Solid State *Adv. Polym. Sci.* **212**, 227-272 (2008).

26. Chunwaschirasiri, W., Tanto, B., Huber, D.L. & Winokur, M.J. Chain Conformations and Photoluminescence of Poly(di-n-octylfluorene) *Phys. Rev. Lett.* **94**, 107402 (2005).
27. Baumgarten, J.L. Ferrochirality: A simple theoretical model of interacting dynamically invertible helical polymers, 1 The basic effects *Macromol. Rapid Commun.* **15**, 175-182 (1994).
28. Sato, T., Terao, K., Teramoto, A. & Fujiki, M. On the Composition-Driven Helical Screw-Sense Inversion of Chiral-Achiral Random Copolymers *Macromolecules* **35**, 5355-5357 (2002).
29. Lifson, S., Andreola, C., Peterson, N.C. & Green, M.M. A Statistical Thermodynamic Analysis of the Cooperative Source of Helix Sense Preference in Polyisocyanates: The Amplification of a Conformational Equilibrium Deuterium Isotope Effect *J. Am. Chem. Soc.* **111**, 8850-8858 (1989).
30. Gu, H., Sato, T., Teramoto, A., Varichon, L. & Green, M.M. Molecular Mechanisms for the Optical Activities of Polyisocyanates Induced by Intramolecular Chiral Perturbations *Polym. J.* **29**, 77-84 (1997).
31. Gu, H., Nakamura, Y., Sato, T., Teramoto, A., Green, M.M., Jha, S.K., Andreola, C. & Reidy, M.P. Optical Rotation of Random Copolyisocyanates of Chiral and Achiral Monomers: Sergeant and Soldier Copolymers *Macromolecules* **31**, 6362-6368 (1998).

32. Morino, K., Maeda, K., Okamoto, Y., Yashima, E. & Sato, T. Temperature Dependence of Helical Structures of Poly(phenylacetylene) Derivatives Bearing an Optically Active Substituent *Chem. Eur. J.* **8**, 5112-5120 (2002).
33. Sato, T., Terao, K., Teramoto, A. & Fujiki, M. Molecular Properties of Helical Polysilylenes in Solution *Polymer* **44**, 5477-5495 (2003).

Chapter 4.

X-Ray Scattering Study on Concentrated Solutions of Polyfluorene Derivatives

4.1 Introduction

In the preceding Chapters, I found the induction of circular dichroism (CD) in phase-separating solutions of optically active polyfluorenes. The phase-separating solutions contain mesoscopic droplets of the concentrated phase, of which concentration is as high as 0.5 g/cm^3 , and it was concluded that the CD induction occurs in the concentrated phase due to chiral interaction among polyfluorene chains. Although the information of the concentrated droplet phase was taken by light scattering, it was difficult to investigate the internal structure of the concentrated phase where polymer chains interact each other.

In this Chapter, the static structure factor of polyfluorene derivative chains in uniform concentrated solutions was studied by X-ray scattering. The static structure factor reflects the intermolecular packing structure of polymer chains that would help to obtain the information of the detailed mechanism of the CD induction.

4.2 Experimental Section

4.2.1 Polymer Samples

The chiral-achiral random copolymer samples PC5O5 and PC2O8 were used in this Chapter. Molecular characteristics of the samples are listed in Table 3-I.

4.2.2 Preparation of Dilute THF Solutions

Dilute THF solutions of sample PC5O5 with concentrations from 0.714×10^{-2} to 1.39×10^{-2} g/cm³ were first examined to check the conformation of the copolymer in THF. The solutions were filled into a quartz capillary cell with a pass length of 2 mm.

4.2.3 Preparation of a Precipitate from a Methanol-Added THF Solution

Methanol was added to a THF solution of PC5O5 with a concentration 1.39×10^{-2} g/cm³ to make $\phi_{\text{MeOH}} = 0.51$. Since the copolymer concentration was higher than those used in Chapter 3, the concentrated phase precipitated from the mother solution. Although the copolymer concentration of the precipitate was not measured, it was expected to be as high as 0.5 g/cm³ from the light scattering results described in Chapter 3. The precipitate was quickly collected and sandwiched by two cover glasses to use XS measurements. The sample thickness was about 58 μm .

4.2.4 Preparation of Concentrated Mesitylene Solutions

To prepare a concentrated solution of PC5O5 with a definitely known copolymer concentration, a less volatile solvent mesitylene (b.p.: 165 °C) was added to a dilute THF solution of PC5O5 with $1.79 \times 10^{-2} \text{ g/cm}^3$ and then THF was evaporated at 40 °C under reduced pressure for 6 h. The final light yellow solution without smelling of THF had a copolymer concentration of 0.54 g/cm^3 . The mesitylene solution was sandwiched by two cover glasses with spacer (mending tape) with a thickness of 58 μm to use XS measurements.

A concentrated mesitylene solution of sample PC2O8 was also prepared in the same way. When the copolymer concentration was as high as 0.5 g/cm^3 , the solution became gel without fluidity, probably due to the high content of easily crystallized octyl fluorene units. This gel was set on a sample holder to measure the X-ray scattering intensity.

4.2.5 X-ray Scattering

X-ray scattering (XS) measurements were carried out using a synchrotron X-ray radiation with a wavelength of 0.1 nm of SPring-8 as the light source and a 30 cm \times 30 cm imaging plate (Rigaku R-AXIS VII) as the detector. The detector camera was set at 1.6 m ($k < 5 \text{ nm}^{-1}$) was used for dilute solutions and 0.3 m ($k < 30 \text{ nm}^{-1}$) distant from the sample cell for the others.

4.2.6 CD and UV-VIS Measurements

CD and UV-vis measurements were carried out for a concentrated mesitylene solution of sample PC5O5 with a JASCO J-820 spectropolarimeter. The concentrated solution was sandwiched by two round quartz plates with spacer (mending tape) with a thickness of 58 μm . Because of turbidity, it was difficult to increase the cell thickness at CD measurements for concentrated mesitylene solution.

4.3 Results and Discussion

4.3.1 CD and UV-VIS Spectra of the Concentrated Solution

Figure 4-1 shows CD and UV-vis spectra of a concentrated mesitylene solution of PC5O5 with $c = 0.54 \text{ g/cm}^3$ (solid curves). Since the solution was slightly turbid, ϵ may increase at shorter wavelength due to light scattering. Furthermore, because of weak signal, the S/N ratio of the CD spectrum is quite low. Taking into account these experimental difficulties, we compare the data with those of the phase-separating THF-methanol solution of the same sample (dashed curves) already shown in Figure 3-2 of Chapter 3. The disagreement in UV-vis spectrum may be mostly owing to the effect of light scattering. Although the CD signal fluctuates considerably, the spectrum at longer wavelengths resembles that for the phase-separating solution. The missing of the positive peak around 350 nm for the mesitylene solution may be due to the strong scattering of the

incident light, which makes the CD measurement more difficult.

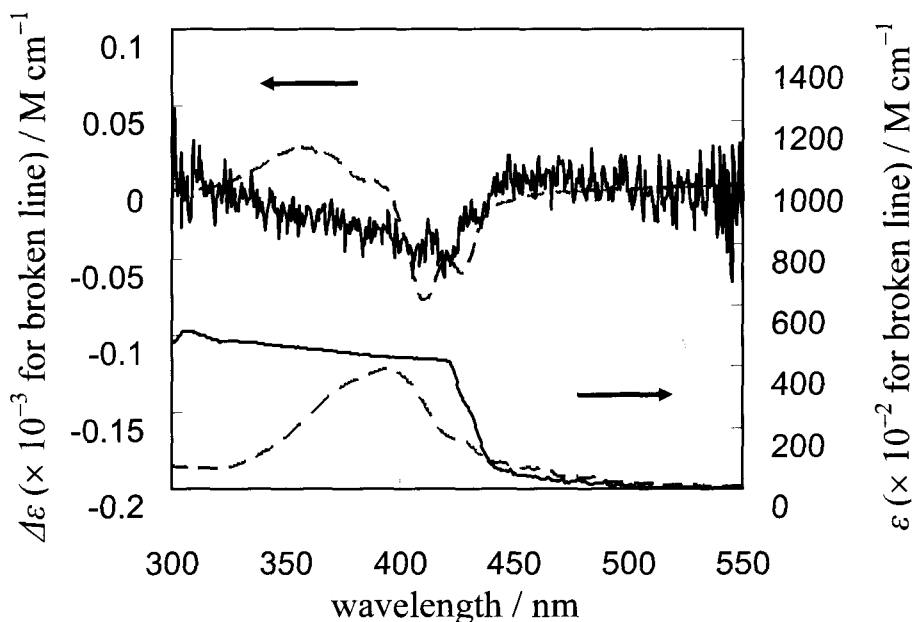


Figure 4-1. CD and UV-vis spectra of a concentrated mesitylene solution of sample PC505 compared with those of a phase-separating THF-methanol solution of the same sample.

4.3.2 X-ray Scattering Profiles

(a) Dilute THF Solutions

Figure 4-2 shows X-ray scattering profiles of dilute THF solutions of sample PC505. Here, the ordinate is the intensity $I(k)$ of the scattered X-ray normalized by the copolymer concentration c , and the abscissa is the magnitude of the scattering vector k defined as $k = (4\pi / \lambda) \sin(\theta / 2)$ with the scattering angle θ and wavelength λ . The intensities sharply decrease with k ,

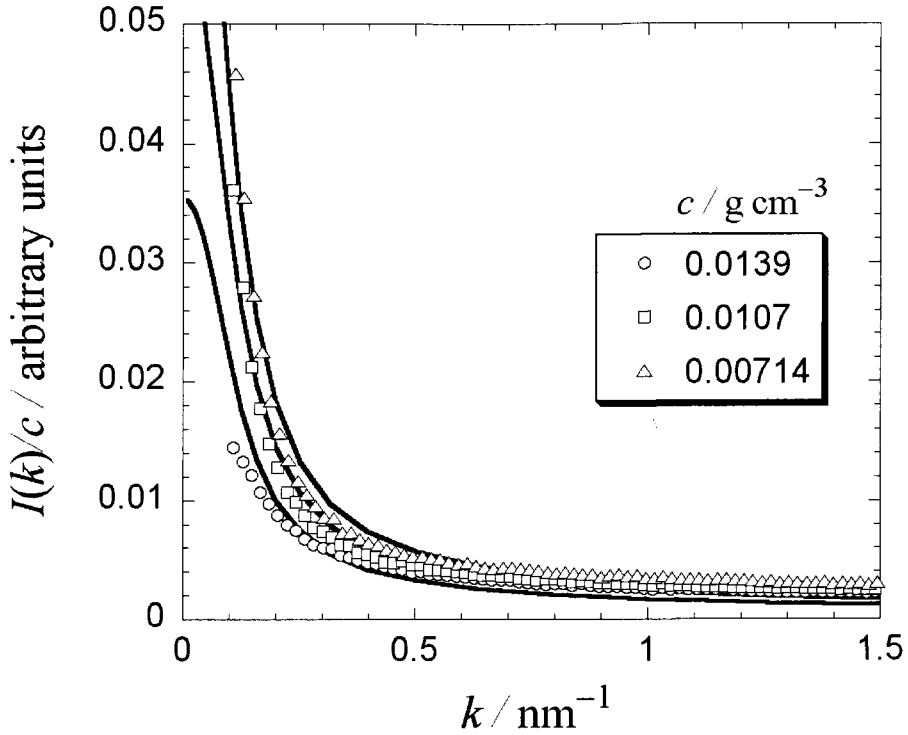


Figure 4-2. XS profiles of dilute THF solutions of sample PC5O5 compared with theoretical curves of the wormlike chain with $q = 8 \text{ nm}^{-1}$ and $M_L = 530 \text{ nm}^{-1}$.

due to the intramolecular interference effect. The scattering intensity $I(k)$ from dilute polymer solutions may be expressed as

$$\frac{I(k)}{c} = \frac{\tilde{K}M_w P(k)}{1 + 2M_w P(k)A_2 c} \quad (1)$$

where \tilde{K} is a optical constant, and M_w , $P(k)$, and A_2 are the weight average molecular weight the intramolecular interference factor, and the second virial coefficient, respectively of the polymer.

Yamakawa and Yoshizaki calculated $P(k)$ for the helical wormlike chain.¹ Their theoretical $P(k)$ contains the persistence length q and the molar mass per unit contour length M_L as parameters in the wormlike chain limit. Wu et al. determined the parameters for poly(2,7-[9,9-bis((S)-3,7-dimethyloctyl)]fluorine) (PDMOF) in THF from the molecular weight dependence of the intrinsic viscosity.² Using the same wormlike chain parameters ($q = 8$ nm and $M_L = 530$ g mol⁻¹ nm⁻¹) as well as $M_w = 7.0 \times 10^4$ (cf. Table 3-I) and $A_2 = 5 \times 10^{-4}$ cm³ mol g⁻², we have calculated $I(k)$ from Eq. (1) where \bar{k} were chosen to obtain the best fit to the experimental results. The solid curves in Figure 4-2 indicate the theoretical values of $I(k)/c$ for the three c , and agreements between theory and experiment are reasonably well. This implies that the conformation of the copolymer PC5O5 resembles that of PDMOF in the same solvent THF.

(b) Concentrated Solutions

Figure 4-3 shows the X-ray scattering profile for the precipitate taken from a methanol-added THF solution of sample PC5O5. The profile has a sharp peak at $k = 4.16$ nm⁻¹, and also a small peak at $k = 3.77$ nm⁻¹. The sharp peaks imply a crystalline ordering. However, after the XS measurement, where strong X-ray was irradiated for 180 s, the sample was dried by heat due to the X-ray irradiation. The copolymer PC5O5 may crystallize during the drying process.

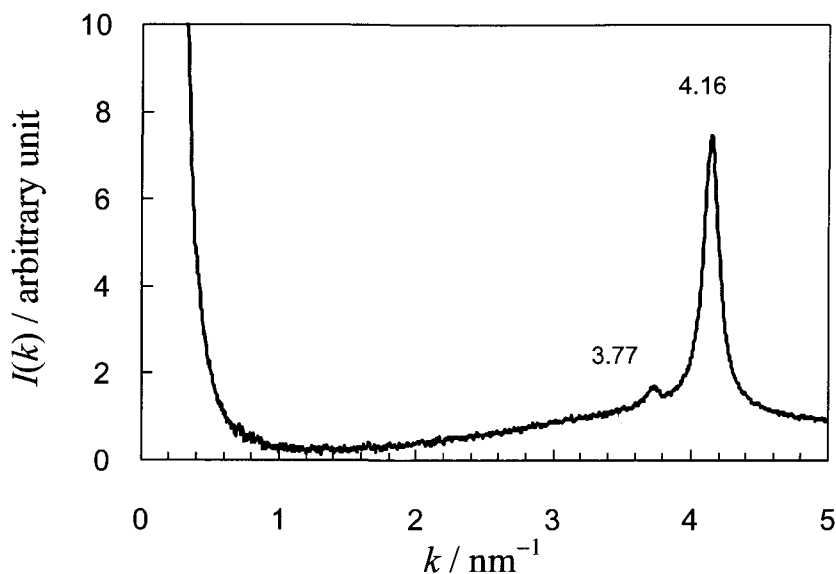


Figure 4-3. XS profiles of a precipitate of PC5O5 from THF solution.

To make XS measurements of the concentrated solution with a definitely known concentration, we changed the solvent from THF to a less volatile solvent mesitylene. Figure 4-4 shows the XS pattern for a concentrated mesitylene solution of sample PC5O5 with $c = 0.54 \text{ g/cm}^3$. We observe two broad peaks around $k = 11.5$ and 15.6 nm^{-1} . The broad peaks may reflect a liquid-like packing structure of the polyfluorene chain in the concentrated solution. The average distance between neighboring polyfluorene chains (i.e., the peak position of the radial distribution function) may be calculated from Bragg's equation $d = 2\pi/k$. The two peaks give us $d = 0.55 \text{ nm}$ ($k = 11.5 \text{ nm}^{-1}$) and 0.40 nm ($k = 15.6 \text{ nm}^{-1}$).

Based on molecular modeling based on *ab initio* MO calculations, Lieser et al. proposed a 5/2 helix model for poly(9,9-bis(2-ethylhexyl)fluorene) (PF2/6) with branched alkyl side chains.³ They estimated the average diameter of the helix to be ca. 1.6 nm. This diameter is close to the hydrodynamic thickness (= 1.45 nm) of poly(2,7-[9,9-bis((*S*)-3,7-dimethyloctyl)]fluorene) (PDMOF) in THF obtained by Wu et al.² from the molecular weight dependence of the intrinsic viscosity. Those polymer chain diameters are considerably larger than the inter-chain distance d obtained above from XS for PC5O5.

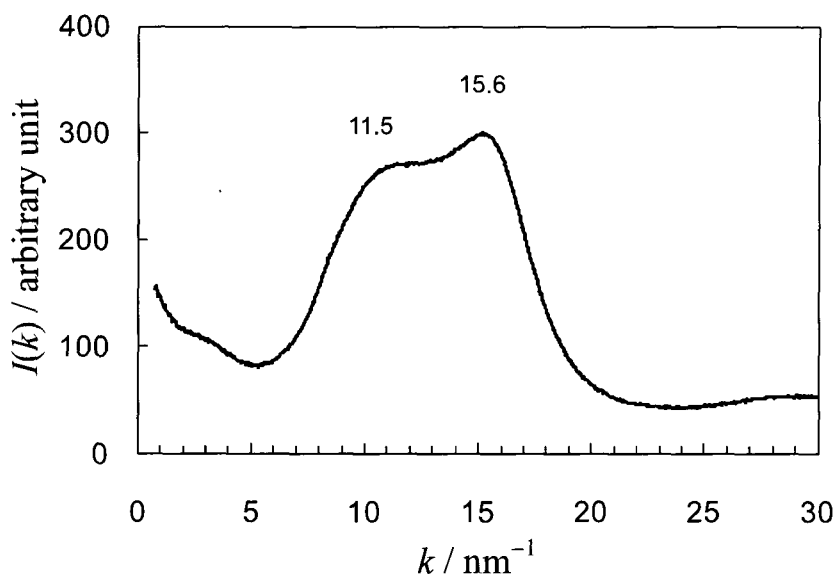


Figure 4-4. XS profiles of PC5O5 concentrated sample condensed from PC5O5-mesitylene mixture.

Chen et al. analyzed a single crystal data of poly(9,9-di-*n*-octylfluorene) (PF8) with linear alkyl side chains to propose a crystalline structure^{4,5} where side chains of neighboring polyfluorene chains interpenetrate each other and the distance between the neighboring main chains is much shorter than the diameter of the individual chain (cf. Figure 3a of ref. 5). Later, Knaapila et al. studied the crystalline and liquid-crystalline states of PF2/6 with different molecular weights.⁶ Using the unit cell dimension and the number of chains per unit cell, they estimated the mean area per chain σ in the crystalline and liquid-crystalline states. The mean inter-chain distance d calculated by $d = \sigma^{1/2}$ was 0.86 nm and 0.97 nm in the crystalline and liquid-crystalline states, respectively. Although the d values are larger than those obtained from the scattering pattern of concentrated PC5O5 solution, but still smaller than the diameter of the PF2/6 chain.

Although we do not have enough information about the side-chain conformation in solution, the inter-chain distance values d obtained above indicate that two polyfluorene derivative chains can approach each other by escaping the collision among side chains.

We have further studied a concentrated mesitylene solution of sample PC2O8 by a XS measurement. The scattering pattern of the solution displayed in Figure 4-5 possesses a few sharp peaks; the sharpest peak at 5 cm^{-1} may correspond to the peak at 4.2 nm^{-1} in Figure 4-3. These sharp

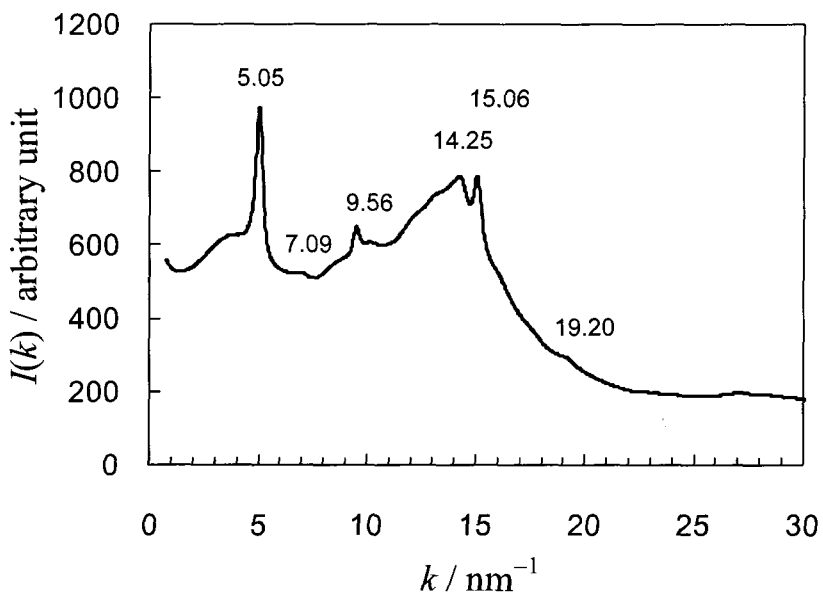


Figure 4-5. XS profiles of a concentrated mesitylene solution of PC2O8.

peaks indicate a crystalline ordering in the solution, In fact, the solution was a gel and PC2O8 chains in the solution may partially crystallize to form a network because of the easily crystallized di-octyl fluorene unit. The X-ray powder diffraction profile of PF8 obtained by Chen et al. has strong peaks at 3.7 nm^{-1} , 4.8 nm^{-1} , 7.8 nm^{-1} , 11 nm^{-1} , and 15 nm^{-1} , and more recently Faria et al. reported similar diffraction pattern of the same polymer.⁷ Among the peaks, some correspond to the peaks of PC2O8, indicating that the packing structure in the crystalline domain of PC2O8 resembles that of crystalline PF8. In the scattering profile of PC2O8

solution, broad peaks around 10 and 15 nm⁻¹ similar to those for PC5O5 (Figure 4-4) are overlapped with the sharp peaks. This indicates that the liquid-like packing structure remains also in the PC2O8 solution. The peak positions indicate a close approach of neighboring PC2O8 chains by escaping the collision among side chains.

4.4 Conclusion

We investigated the packing structure of chiral-achiral random copolymer chains PC5O5 and PC2O8 in concentrated solutions and a gel, respectively, by X-ray scattering. Our conclusion is that neighboring chains can closely approach each other by escaping the collision among side chains. If the side chains might wrap the polyfluorene backbone and two chains could not come close in solution, we might not expect the intermolecular chiral interaction among side chains and polyfluorene backbone belonging to different chains. Since the intermolecular chiral interaction is essential to the mechanism of the phase-separation induced CD phenomenon proposed in the preceding Chapters. Therefore, the XS evidence for close approaching of the neighboring chains is consistent with our CD induction mechanism.

4.5 References

- 1 Yoshizaki, T., Nitta, I. & Yamakawa, H. Transport coefficients of helical wormlike chains. 4. Intrinsic viscosity of the touched-bead model. *Macromolecules* **21**, 165-171 (1988).
- 2 Wu, L., Sato, T., Tang, H.-Z. & Fujiki, M. Conformation of a Polyfluorene Derivative in Solution. *Macromolecules* **37**, 6183-6188 (2004).
- 3 Lieser, G., Oda, M., Miteva, T., Meisel, A., Nothofer, H.-G., Scherf, U. & Neher, D. Ordering, Graphoepitaxial Orientation, and Conformation of a Polyfluorene Derivative of the “Hairy-Rod” Type on an Oriented Substrate of Polyimide. *Macromolecules* **33**, 4490-4495 (2000).
- 4 Chen, S. H., Su, A. C. & Chen, S. A. Noncrystalline Phases in Poly(9,9-di-n-octyl-2,7-fluorene). *The Journal of Physical Chemistry B* **109**, 10067-10072 (2005).
- 5 Chen, S. H., Chou, H. L., Su, A. C. & Chen, S. A. Molecular Packing in Crystalline Poly(9,9-di-n-octyl-2,7-fluorene). *Macromolecules* **37**, 6833-6838 (2004).
- 6 Knaapila, M., Stepanyan, R., Lyons, B. P., Torkkeli, M. & Monkman, A. P. Towards General Guidelines for Aligned, Nanoscale Assemblies of Hairy-Rod Polyfluorene. *Advanced Functional Materials* **16**, 599-609 (2006).

- 7 Faria, G. C., Plivelic, T. S., Cossello, R. F., Souza, A. A., Atvars, T. D. Z., Torriani, I. L. & deAzevedo, E. R. A Multitechnique Study of Structure and Dynamics of Polyfluorene Cast Films and the Influence on Their Photoluminescence. *The Journal of Physical Chemistry B* **113**, 11403-11413 (2009).

Chapter 5.

Summary and Conclusions

π -Conjugated polymers exhibit interesting optical and electro-optical properties, which can be utilized as semiconductors, chemical and bio-sensors, displays, and so on. In this thesis, we studied circular dichroism (CD) behavior of optically active polyfluorenes induced along with the phase separation in dilute solution. The studies are summarized as follows.

Chapter 2. Phase-Separation Induced Circular Dichroism in Dilute Solutions of an Optically Active Polyfluorene Homopolymer

When a non-solvent methanol was added to dilute THF solutions of an optically active polyfluorene derivative, the liquid-liquid phase separation took place, and CD was induced at a low temperature. The polymer concentration of the separating minor phase, estimated by light scattering, was very high ($\sim 0.5 \text{ g/cm}^3$). The CD induction occurring in that concentrated phase was sensitive to the temperature. When the phase-separating solution was quenched from 40 to 10 °C, CD was amplified according to the first-order reaction kinetics, and it was a rather slow process (the rate constant: $2.5 \times 10^{-4} \text{ s}^{-1}$). The intermolecular chiral interaction in the concentrated phase may be responsible for the phase-separating CD induction or non-racemization of this helical

polyfluorene derivative.

Chapter 3. Double Screw-Sense Inversions of Helical Chiral-Achiral Random Copolymers of Fluorene Derivatives in Phase Separating Solutions

The addition of methanol to dilute THF solutions of chiral-achiral random copolymers of fluorene derivatives and the chiral homopolymer showed thermo-reversible CD induction in the main-chain fluorene absorption region, demonstrating the uneven population of the right- and left-handed helical conformation in the polymer chains. From the sign of the induced CD, we found two helical screw-sense inversions by changing the chiral monomer content. The Ising model for chirally interacting chiral-achiral random copolymers can explain the double screw-sense inversions.

Chapter 4. X-Ray Scattering Study on Concentrated Solutions of Polyfluorene Derivatives

Circular dichroism was induced in concentrated phase droplets in phase separated solutions of optically active polyfluorenes as reported in the preceding Chapters. To elucidate the CD induction mechanism in the concentrated phase, X-ray scattering (XS) measurements were carried out on concentrated mesitylene solutions of optically active polyfluorenes in this Chapter. The XS profile for a concentrated mesitylene solution of a chiral-achiral random copolymer PC5O5 has

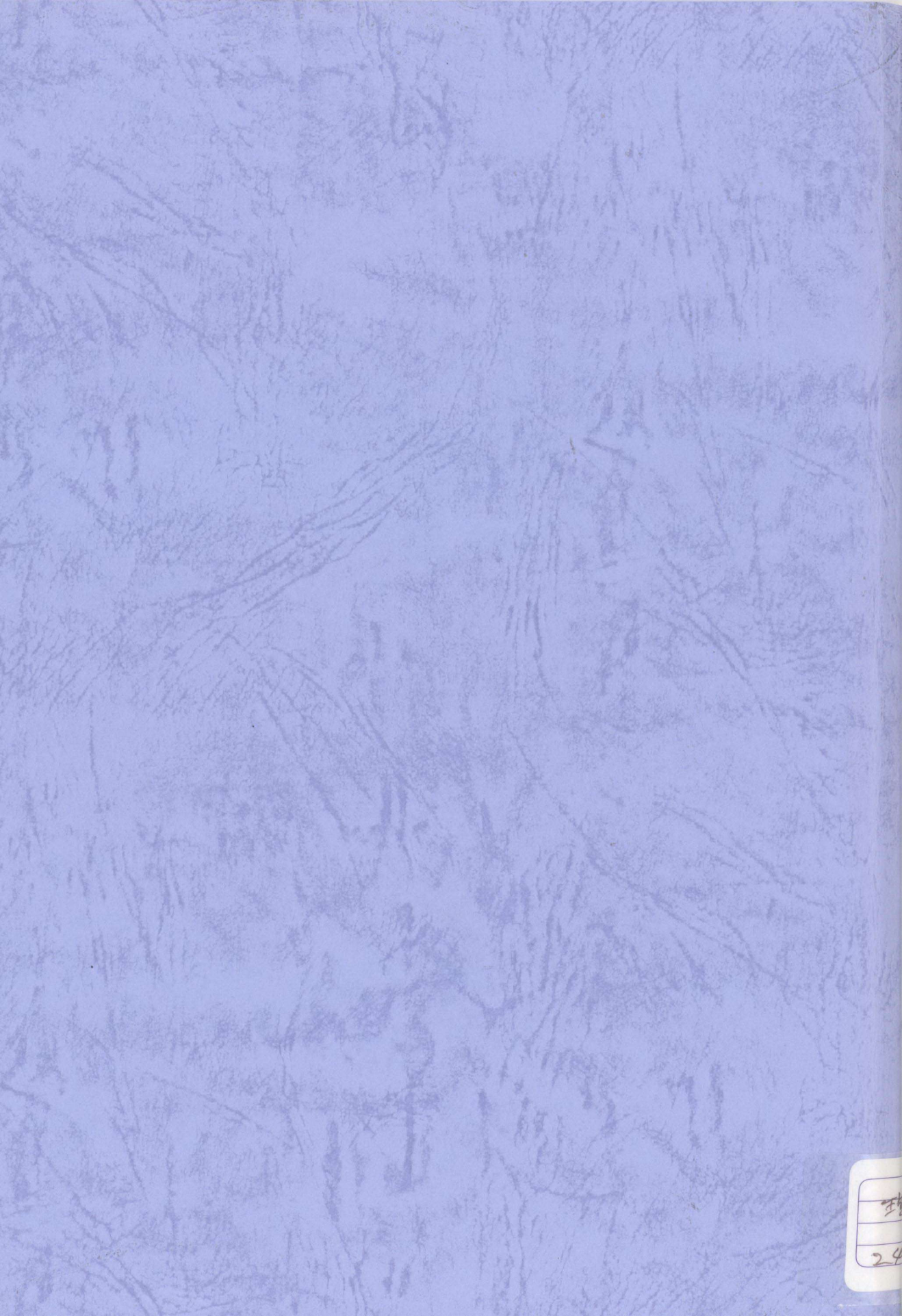
broad peaks around the magnitude of the scattering vector $k = 11.5$ and 15.6 nm^{-1} , which correspond to the inter-chain distances $d = 0.55 \text{ nm}$ and 0.40 nm , being considerably smaller than the average thickness of the polyfluorene chain. Although we do not have enough information about the side-chain conformation in solution, the inter-chain distance values d obtained indicate that two polyfluorene derivative chains in concentrated solution can approach each other by escaping the collision among side chains, which is prerequisite for the intermolecular chiral interaction among side chains and polyfluorene backbone belonging to different chains.

Optically active polythiophene and polysilane derivatives are famous examples exhibiting aggregation- and phase-separation-induced CD. However, the detailed mechanism of the CD induction has not been elucidated so far. The results obtained in the present study for optically active polyfluorene derivatives may help to understand the aggregation- and phase-separation-induced CD for the other conjugated polymers.

List of Publications

This thesis work has been or will be published in the following papers.

- 1 Sanada, Y. & Sato, T. Induced circular dichroism of an optically active polyfluorene derivative in phase-separating solutions. *Polymer Journal*, **42**, 195-200 (2010).
- 2 Sanada, Y., Terao, K., & Sato, T. Double screw-sense inversions of helical chiral-achiral random copolymers of fluorene derivatives in phase separating solutions, *Polymer Journal*, in press.
- 3 Sanada, Y., Sakurai, K., & Sato, T. X-Ray Scattering Study on Concentrated Solutions of Polyfluorene Derivatives, in preparation.



24
24